

## Article

# Study on Heat Storage Performance of Phase Change Reservoir in Underground Protection Engineering

Hongyu Zhang<sup>1</sup>, Fei Gan<sup>1</sup>, Guangqin Huang<sup>1</sup>, Chunlong Zhuang<sup>1</sup>, Xiaodong Shen<sup>1</sup>, Shengbo Li<sup>1,\*</sup>, Lei Cheng<sup>1</sup>, Shanshan Hou<sup>1</sup>, Ningge Xu<sup>1</sup> and Zhenqun Sang<sup>2</sup>

<sup>1</sup> Department of Military Installation, Army Logistics Academy of PLA, Chongqing 401331, China

<sup>2</sup> School of Communication Sergeant, Army Engineering University of PLA, Chongqing 400035, China

\* Correspondence: cqlsb\_112@163.com; Tel.: +86-138-832-91029

**Abstract:** In view of the main problems of the condensing heat discharge modes of the existing underground air-conditioning system, the technical scheme of using phase change heat storage modules to improve the heat storage capacity of the reservoir is proposed. By establishing a 3D flow and transient heat transfer model of the phase change reservoir, the effects of thermal property parameters, package size and arrangement of the phase change heat storage modules on the heat storage performance of the phase change reservoir were quantitatively analyzed based on three indexes: heat storage capacity per volume  $\Delta q$ , guaranteed efficiency coefficient  $\eta$  and slope of temperature rise per unit load  $\varepsilon$ . The results show that when the phase change temperature is 29 °C (23 °C increased to 33 °C) and the latent heat value is 250 kJ/kg (100 kJ/kg increased to 250 kJ/kg),  $\Delta q$  (110.92 MJ/m<sup>3</sup>, 112.83 MJ/m<sup>3</sup>) and  $\eta$  (1.22, 1.24) under both conditions are at their most, respectively, indicating that the phase change temperature should be less than 4 °C at the outlet temperature of the reservoir, and phase change materials with a high latent heat should be selected in engineering design whenever possible. When the size of the phase change module is 150 mm × 20 mm and the phase change reservoir adopts four intakes,  $\varepsilon$  (0.259, 0.244) under both conditions is the smallest, indicating that increasing the area of the phase change heat storage module and the fluid and increasing the inlet disturbance of the reservoir can enhance its heat storage capacity.

**Keywords:** underground protection engineering; air-conditioning reservoir; phase change material; phase change heat storage



**Citation:** Zhang, H.; Gan, F.; Huang, G.; Zhuang, C.; Shen, X.; Li, S.; Cheng, L.; Hou, S.; Xu, N.; Sang, Z. Study on Heat Storage Performance of Phase Change Reservoir in Underground Protection Engineering. *Energies* **2022**, *15*, 5731. <https://doi.org/10.3390/en15155731>

Academic Editors: Xiaohu Yang and Kamel Hooman

Received: 11 July 2022

Accepted: 5 August 2022

Published: 7 August 2022

**Publisher's Note:** MDPI stays neutral with regard to jurisdictional claims in published maps and institutional affiliations.



**Copyright:** © 2022 by the authors. Licensee MDPI, Basel, Switzerland. This article is an open access article distributed under the terms and conditions of the Creative Commons Attribution (CC BY) license (<https://creativecommons.org/licenses/by/4.0/>).

## 1. Introduction

In recent years, with the rapid increase in electronic equipment and terminals, the waste heat in underground protection engineering has upsurges, which results in a region of high thermal density [1,2]. When engineering is in a general protection state, the condensing heat generated by the ventilation and air-conditioning system is transported to the outside by the cooling tower. This external cooling tower has poor concealment and weak protection. It is very easy to cause infrared exposure and visible light exposure. When underground engineering is in isolated states in wartime, the condensing heat is stored in a large reservoir set inside. However, a longtime operation will lead to the rise of the reservoir temperature and reduce the continuous support ability of the ventilation and air-conditioning system to the internal environment of the engineering [3]. Therefore, it is of great significance to adopt the appropriate technology to improve the heat storage capacity of the reservoir and replace the outside cooling tower of the system without increasing the volume of the reservoir. The technical scheme aims to prolong the operation time of the air-conditioning system, avoid infrared exposure and improve the reliability of the system.

To solve the problems of concealment, protection and reliability in condensing the heat treatment mode in traditional underground protective engineering, researchers have carried out a lot of schemes for the replacement of cooling towers in the system, the

improvement of cooling towers in the ground and the development of new condensing heat discharge devices. Wang Jinsheng et al. [4] proposed the model of an underground storage cooling tower. The cooling tower was placed above the underground reservoir, and the waste heat was removed by the evaporation of water from the reservoir and by air intake and exhaust from the diesel power station. He Yecong et al. [5] developed a rotary spray indirect evaporative cooler according to the characteristics of subway operation. This kind of cooler can be installed in the exhaust channel of underground buildings to replace existing external cooling towers. Liu Yingyi et al. [6] moved the cooling tower to the exhaust fan room near the underground air-conditioning room in the design of the air-conditioning system of an actual underground protective engineering. They used the engineering exhaust air and part of the fresh air as cooling air sources. Nevertheless, the disadvantage is that the above schemes require the additional introduction of fresh air as the exhaust air of the cooling tower and increased the size of the air duct and the operating cost. To solve the problem of the vulnerable deficiencies of the cooling tower and based on the fact that the water temperature of underground projects is stable at 7–26 °C all year round, Geng Shibin et al. [7] proposed a combination mode of underground water storage reservoirs and air-cooled heat pump units to replace cooling towers because of the shortcomings of the traditional cooling tower. Aiming at the exposure characteristics of the ground cooling tower, Zhang Hua et al. [8] proposed the ground source dehumidifying and air-conditioning system. The system improved the protective capability of civil engineering, which had the function of temperature adjustment and heat pump, and it could run in a different mode with a different capacity unit, which could satisfy the different needs of civil engineering in maintenance or wartime. Mao Jinfeng et al. [9,10] used buried tube heat exchangers to discharge heat into the rock and soil. Their study focused on the heat transfer performance of buried tube heat exchangers to improve the condensing heat discharge capacity. Fei Chen et al. [11] researched the energy efficiency of U-shaped buried tube heat exchangers, by using phase change materials (PCMs) as grouting materials in the backfill area and analyzed the effects of physical parameters and operation modes on the energy efficiency of ground source heat pumps.

Among all the above technical schemes, the scheme of installing the underground cooling tower only reduces the infrared exposure point of the project but does not fundamentally solve the infrared exposure problem. In other schemes, the use of the water loop heat pump to transfer heat does not transfer the heat out of engineering. However, the water loop heat pump has high demands on the site of the engineering and inner load distribution. The water loop heat pump system's ability to control humidity underground is limited at the same time. The condensing heat discharge scheme of the buried pipe heat exchanger has problems such as deep drilling holes and easy thermal short circuits. Therefore, the scheme of using a cooling reservoir to store condensation heat instead of the cooling tower is still an effective technique to solve the concealment problem in underground protection engineering. Under this circumstance, improving the heat storage capacity of the reservoir is an effective idea to improve the continuous operation capacity of the internal air-conditioning system of the project.

As a favorable medium for energy storage, PCMs have the advantages of high heat storage density, large heat storage capacity, low cost and good chemical stability [12], which are widely used in various applications including buildings [13,14], process heat [15], concentrated solar power (CSP) plants [16–18] or solar cooling [19,20] and thermal energy storage [21,22]. Mingkan Zhang et al. [23,24] proposed an innovative underground heat exchanger which consisted of a water-filled tank that also contained a PCM to improve the thermal storage capacity. The simulation results indicated that the underground heat exchanger can better regulate the entering water temperature of a ground source heat pump than a conventional vertical bore ground heat exchanger under short-term high thermal load conditions, which has a better operating efficiency. Yanjun Zhang et al. [25] constructed a shell heat storage device with a stirrer inside to strengthen the heat transfer performance of the PCM. The results showed that the average charging rate increased by 32.23 J/s than that

without stirring, and the average discharging rate increased by 47.39 J/s. The completion time for charging/discharging with stirring was shortened by 9.61% and 48.61% than that without stirring. Georg Scharinger-Urschitz et al. [26] conducted experimental research on the thermal energy storage system with PCMs and quantified the heat transfer performance of the thermal energy storage devices with different fin structures. Additionally, they analyzed the PCM temperature trends and different melting patterns occurred in the radial and axial directions and in the individual geometry sections based on the enthalpy function. Therefore, it is an effective method to improve the heat storage capacity of a thermal energy storage system by using PCMs. Therefore, the heat capacity can be increased without increasing the existing volume of the reservoir under the condition that appropriate PCMs are selected and applied to the reservoir of the existing underground engineering. In the meantime, the operation time of the air-conditioning system can be prolonged. This is of greater significance when the underground engineering is isolated and protected. Li Hong et al. [27] proposed a scheme of a phase change regenerative air-conditioning cooling reservoir in the protection project. This aimed to enhance the condensing heat treatment capacity of the reservoir and meet the heat discharge requirements of the continuous operation of the system under isolation and protection conditions. This was theoretically proven that adding suitable PCMs to the heat storage reservoir can greatly improve the capacity of the reservoir without increasing the volume of the reservoir. Hou Pumin et al. [28,29] proposed a phase change heat storage reservoir to deal with the waste heat of underground engineering power stations. Meanwhile, through experimental studies, the influences of the form and size of the heat storage module, heat exchange fluid flow and inlet temperature on the temperature distribution and heat storage rate of the heat storage reservoir were analyzed. Alicia Crespo et al. [30] developed a thermal energy storage tank filled with commercial PCM flat slabs to provide heat at approximately 15 °C to the evaporator of a seasonal thermal energy storage system and optimized the number, type and configuration of slabs to enhance its thermal energy storage capacity.

To further explore the practical application of a phase change reservoir in underground protection engineering to deal with condensing the heat of an air-conditioning system, an experimental platform was built. The influence of the amount of the phase change heat storage module and the flow of cooling water on the heat storage performance of the reservoir under constant load [31] was studied. The heat storage per unit volume  $\Delta q$  and the guaranteed efficiency coefficient  $\eta$  of the reservoir defined based on the outlet temperature are the evaluation indexes of the heat storage performance of the reservoir in underground protection engineering. Due to the limited parameters that can be controlled in the experimental process, it is not possible to carry out a more detailed analysis and research on the various factors that affect its heat storage performance. Additionally, due to actual limitations on the selection of PCMs, the physical properties of materials are not necessarily optimized. Therefore, based on the flow and heat transfer characteristics of the reservoir and the established experimental platform, a three-dimensional flow and the transient heat transfer numerical model of the underground air-conditioning phase change reservoir has been established. The effects of the physical properties of the PCM, the structure size of the phase change heat storage module and the water distribution on the heat storage performance of the phase change reservoir are analyzed.

## 2. Experimental Heat Storage System of Air-Conditioning Phase Change Cooling Reservoir

The experimental heat storage system of a phase change cooling reservoir for underground air-conditioning was described in previous research [31]: it consists of condensing the heat load module of the air-conditioning system, a phase change cooling reservoir heat storage module and an experimental test module. The system schematic diagram is shown in Figure 1. The components of each module are as follows:

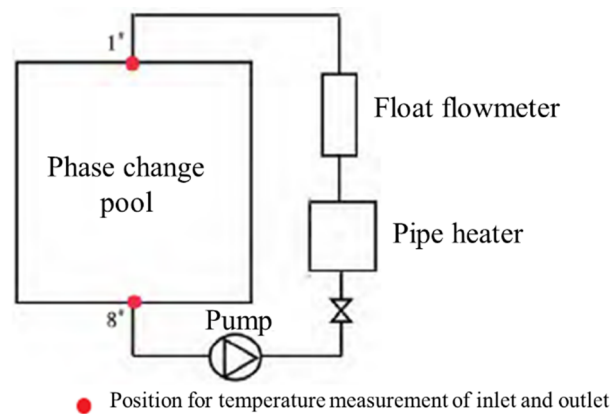


**Figure 1.** Schematic diagram of experimental heat storage system for phase change cooling reservoir of air-conditioning.

Condensing the heat load module of a system mainly consists of the pipe heater and the circulating water pump. The heat generated by the pipe heater is used to simulate the condensing heat load of the system. The circulating water pump provides the power of circulation. The pipe heater used in the experiment has a rated power of 2 kW. The pump is a German Welle pipe circulating pump with a rated pump head of 5 m and a rated flow of 13 L/min. The inlet and outlet water flows are regulated by the circulating pump's three-gear power adjustment switch and the valve on the pipeline.

The heat storage module of the phase change reservoir is mainly composed of a reservoir, phase change heat storage module and a bracket. The reservoir is poured on-site with cement concrete, and its dimensions are length  $\times$  width  $\times$  height = 1300 mm  $\times$  1300 mm  $\times$  1200 mm. The water distribution mode is from top to bottom, and the inlet and outlet are in the center of the upper and lower surfaces of the reservoir. During the experiment, the reservoir was insulated and the effective volume of the reservoir was 1.86 m<sup>3</sup>. The packaging form of the PCM was strip. Stainless steel was used as the packaging material considering the corrosion and the high thermal conductivity of PCM. The dimensions of the package stainless steel are 1100 mm  $\times$  100 mm  $\times$  30 mm. The liquid PCM was injected into hollow strip stainless steel to form a phase change heat storage module. The encapsulated phase change heat storage module is shown in Figure 2a. The bracket was used to place the phase change heat storage module. A total of four layers were set from the bottom of the reservoir upward, and six modules were arranged in each layer. The height of the bracket of each layer is shown in Table 1, and each layer has 0.19 m between each other. The final phase change reservoir heat storage module is shown in Figure 2b.



**Figure 2.** Physical test bench. (a) The appearance of the reservoir; and (b) The arrangement of the phase change module.

**Table 1.** Setting the height of each layer of the bracket.

The Number of Layers	The First Layer	The Second Floor	The Third Layer	The Fourth Floor	The Fifth Floor	The Sixth Layer
Height (m)	0.12	0.31	0.5	0.69	0.88	1.07

### 3. Three-Dimensional Flow and Transient Heat Transfer Model of Phase Change Reservoir

#### 3.1. Establishment of Governing Equations for Phase Change Reservoir

The flow and heat transfer of the phase change heat storage reservoir in underground engineering air-conditioning mainly includes three processes: water flow and heat transfer in the reservoir; heat transfer in the phase change module; and the unsteady heat transfer of the reservoir wall. To simplify the model, the following assumptions were adopted in the modeling process:

- (1) The water body is considered an incompressible fluid. This means that the density change caused by temperature is not considered;
- (2) The unsteady effect of water flow is ignored. This means that the water flow field does not change during the whole flow and heat transfer process;
- (3) The physical properties of PCM are independent of temperature;
- (4) The volume change of solid and liquid phases of PCM is ignored.

For water the flow in the phase change reservoirs, the classical k- $\epsilon$  two-equation model is used to describe the turbulent velocity field of water. The unsteady energy conservation equation considering water flow is used for heat transfer. The unsteady heat conduction model is used for the heat transfer of the reservoir surface. In this research, the sensible heat capacity method [32] is adopted for the phase change module in the module of the reservoir to simulate the phase change heat transfer process. Only the heat conduction process exists for the reservoir surface, so the differential equation of the heat conduction of the constant physical properties without an internal heat source can be directly established.

Firstly, the water flow and heat transfer model in the reservoir is established, and the mass conservation equation is:

$$\frac{\partial \rho}{\partial t} + \frac{\partial \rho u}{\partial x} + \frac{\partial \rho v}{\partial y} + \frac{\partial \rho w}{\partial z} = 0 \quad (1)$$

The momentum conservation equations of the reservoir are:

$$\frac{\partial(\rho u)}{\partial t} + \frac{\partial(\rho u u)}{\partial x} + \frac{\partial(\rho v u)}{\partial y} + \frac{\partial(\rho w u)}{\partial z} = \frac{\partial}{\partial x}(\eta_{eff} \frac{\partial u}{\partial x}) + \frac{\partial}{\partial y}(\eta_{eff} \frac{\partial u}{\partial y}) + \frac{\partial}{\partial z}(\eta_{eff} \frac{\partial u}{\partial z}) + S_u \quad (2)$$

$$\frac{\partial(\rho v)}{\partial t} + \frac{\partial(\rho u v)}{\partial x} + \frac{\partial(\rho v v)}{\partial y} + \frac{\partial(\rho w v)}{\partial z} = \frac{\partial}{\partial x}(\eta_{eff} \frac{\partial v}{\partial x}) + \frac{\partial}{\partial y}(\eta_{eff} \frac{\partial v}{\partial y}) + \frac{\partial}{\partial z}(\eta_{eff} \frac{\partial v}{\partial z}) + S_v \quad (3)$$

$$\frac{\partial(\rho w)}{\partial t} + \frac{\partial(\rho u w)}{\partial x} + \frac{\partial(\rho v w)}{\partial y} + \frac{\partial(\rho w w)}{\partial z} = \frac{\partial}{\partial x}(\eta_{eff} \frac{\partial w}{\partial x}) + \frac{\partial}{\partial y}(\eta_{eff} \frac{\partial w}{\partial y}) + \frac{\partial}{\partial z}(\eta_{eff} \frac{\partial w}{\partial z}) + S_w \quad (4)$$

$$\frac{\partial(\rho k)}{\partial t} + \frac{\partial(\rho u k)}{\partial x} + \frac{\partial(\rho v k)}{\partial y} + \frac{\partial(\rho w k)}{\partial z} = \frac{\partial}{\partial x}((\eta + \frac{\eta_t}{\sigma_k}) \frac{\partial k}{\partial x}) + \frac{\partial}{\partial y}((\eta + \frac{\eta_t}{\sigma_k}) \frac{\partial k}{\partial y}) + \frac{\partial}{\partial z}((\eta + \frac{\eta_t}{\sigma_k}) \frac{\partial k}{\partial z}) + S_k \quad (5)$$

$$\frac{\partial(\rho \epsilon)}{\partial t} + \frac{\partial(\rho u \epsilon)}{\partial x} + \frac{\partial(\rho v \epsilon)}{\partial y} + \frac{\partial(\rho w \epsilon)}{\partial z} = \frac{\partial}{\partial x}((\eta + \frac{\eta_t}{\sigma_\epsilon}) \frac{\partial \epsilon}{\partial x}) + \frac{\partial}{\partial y}((\eta + \frac{\eta_t}{\sigma_\epsilon}) \frac{\partial \epsilon}{\partial y}) + \frac{\partial}{\partial z}((\eta + \frac{\eta_t}{\sigma_\epsilon}) \frac{\partial \epsilon}{\partial z}) + S_\epsilon \quad (6)$$

$S_u, S_v, S_w, S_k, S_\epsilon$  are source items

$$S_u = -\frac{\partial p}{\partial x} + \frac{\partial}{\partial x}(\eta_{eff} \frac{\partial u}{\partial x}) + \frac{\partial}{\partial y}(\eta_{eff} \frac{\partial v}{\partial x}) + \frac{\partial}{\partial z}(\eta_{eff} \frac{\partial w}{\partial x}) \quad (7)$$

$$S_v = -\frac{\partial p}{\partial y} + \frac{\partial}{\partial x}(\eta_{eff} \frac{\partial u}{\partial y}) + \frac{\partial}{\partial y}(\eta_{eff} \frac{\partial v}{\partial y}) + \frac{\partial}{\partial z}(\eta_{eff} \frac{\partial w}{\partial y}) \tag{8}$$

$$S_w = -\frac{\partial p}{\partial z} + \frac{\partial}{\partial x}(\eta_{eff} \frac{\partial u}{\partial z}) + \frac{\partial}{\partial y}(\eta_{eff} \frac{\partial v}{\partial z}) + \frac{\partial}{\partial z}(\eta_{eff} \frac{\partial w}{\partial z}) \tag{9}$$

$$\frac{\partial(\rho k)}{\partial t} + \frac{\partial(\rho uk)}{\partial x} + \frac{\partial(\rho vk)}{\partial y} + \frac{\partial(\rho wk)}{\partial z} = \frac{\partial}{\partial x}((\eta + \frac{\eta_t}{\sigma_k}) \frac{\partial k}{\partial x}) + \frac{\partial}{\partial y}((\eta + \frac{\eta_t}{\sigma_k}) \frac{\partial k}{\partial y}) + \frac{\partial}{\partial z}((\eta + \frac{\eta_t}{\sigma_k}) \frac{\partial k}{\partial z}) + S_k S_k = \rho G_k - \rho \epsilon \tag{10}$$

$$S_k = \frac{\epsilon}{k} (c_1 \rho G_k - c_2 \rho \epsilon) \tag{11}$$

where,  $u, v$  and  $w$  are the velocities in the  $x; y; z$  direction in the Cartesian coordinate system, m/s.  $\rho$  is the fluid density, kg/m<sup>3</sup>.  $k$  is the turbulent kinetic energy, J.  $p$  is the pressure, Pa.  $\epsilon$  is the turbulence energy dissipation rate.  $\eta_{eff}$  is the effective viscosity coefficient, N·s/m<sup>2</sup>.  $\eta$  is the molecular viscosity coefficient, N·s/m<sup>2</sup>.  $\eta_t$  is the turbulent viscosity coefficient, N·s/m<sup>2</sup>,  $\eta_t = c_\mu \rho k^2 / \epsilon$ .  $\sigma_k$  is the turbulent Prandtl numbers of  $k$ .  $\sigma_\epsilon$  is the turbulent Prandtl numbers of  $\epsilon$ .

The equation to calculate  $G_k$  is:

$$G_k = \frac{\eta_t}{\rho} \left\{ 2 \left[ \left( \frac{\partial u}{\partial x} \right)^2 + \left( \frac{\partial v}{\partial y} \right)^2 + \left( \frac{\partial w}{\partial z} \right)^2 \right] + \left( \frac{\partial u}{\partial x} + \frac{\partial v}{\partial y} \right)^2 + \left( \frac{\partial u}{\partial z} + \frac{\partial w}{\partial x} \right)^2 + \left( \frac{\partial w}{\partial y} + \frac{\partial v}{\partial z} \right)^2 \right\} \tag{12}$$

The energy conservation equation of the reservoir is:

$$\frac{\partial(\rho T)}{\partial t} + \frac{\partial(\rho u T)}{\partial x} + \frac{\partial(\rho v T)}{\partial y} + \frac{\partial(\rho w T)}{\partial z} = \frac{\partial}{\partial x} \left( \left( \frac{\eta}{P_r} + \frac{\eta_t}{\sigma_t} \right) \frac{\partial T}{\partial x} \right) + \frac{\partial}{\partial y} \left( \left( \frac{\eta}{P_r} + \frac{\eta_t}{\sigma_t} \right) \frac{\partial T}{\partial y} \right) + \frac{\partial}{\partial z} \left( \left( \frac{\eta}{P_r} + \frac{\eta_t}{\sigma_t} \right) \frac{\partial T}{\partial z} \right) \tag{13}$$

where  $P_r$  is the Prandtl number.  $\sigma_t$  respectively represents the turbulent Prandtl number of the temperature.

Three coefficients ( $c_1, c_2, c_\mu$ ) and three constants ( $\sigma_k, \sigma_\epsilon, \sigma_t$ ) are introduced into the equations, and their values in the  $k$ - $\epsilon$  model are 1.44, 1.92, 0.09, 1.0, 1.3, and 0.9~1.0, respectively [33]. The heat transfer model of the phase change module is established, and the energy conservation equation of the module is:

$$\rho C_{eq} \frac{\partial T}{\partial t} + \nabla(-k_{eq} \nabla T) = Q \tag{14}$$

where  $\rho$  is the density of PCM, in kg/m<sup>3</sup>;  $C_{eq}$  is equivalent specific heat, in J/kg·K;  $k_{eq}$  is the equivalent thermal conductivity, in W/m·K;  $Q$  is the internal heat source intensity, in W/m<sup>3</sup>.

$$\rho = \theta \rho_{ph1} + (1 - \theta) \rho_{ph2} = \theta_1 \rho_{ph1} + \theta_2 \rho_{ph2} \tag{15}$$

$$C_{eq} = \frac{1}{\rho} (\theta_1 \rho_{ph1} C_{Pph1} + \theta_2 \rho_{ph2} C_{Pph2}) \tag{16}$$

$$k_{eq} = \theta_1 k_{ph1} + \theta_2 k_{ph2} \tag{17}$$

$\theta$  is the solid-phase ratio of PCM,  $\theta = \theta_1, \theta_2 = 1 - \theta_1, \theta = \begin{cases} 1 & T < T_{PC} - \frac{\Delta T}{2} \\ 0 & T > T_{PC} + \frac{\Delta T}{2} \end{cases}$ , where  $T_{PC}$  is the phase change temperature of PCM, in °C;  $\Delta T$  is the phase change temperature range, in °C.

$$C_P = \frac{\partial H}{\partial T} \tag{18}$$

$H$  is the enthalpy of PCM:

$$H = \frac{1}{\rho} [\theta \rho_{ph1} H_{ph1} + (1 - \theta) \rho_{ph2} H_{ph2}] \tag{19}$$

Define  $\alpha_m = \frac{1}{2} \frac{\theta_2 \rho_{ph2} - \theta_1 \rho_{ph1}}{\rho}$ , then Formula (18) can be expressed as:

$$C_P = \frac{\partial H}{\partial T} = \frac{1}{\rho} (\theta_1 \rho_{ph1} C_{P_{ph1}} + \theta_2 \rho_{ph2} C_{P_{ph2}}) + (H_{ph1} - H_{ph2}) \frac{d\alpha_m}{dT} \quad (20)$$

Define  $C_L(T) = (H_{ph2} - H_{ph1}) \frac{d\alpha_m}{dT}$ , then Equation (20) can be further expressed as:

$$C_P = \frac{1}{\rho} (\theta_1 \rho_{ph1} C_{P_{ph1}} + \theta_2 \rho_{ph2} C_{P_{ph2}}) + C_L \quad (21)$$

$C_L(T)$  can be approximated as:

$$C_L(T) = L \frac{d\alpha_m}{dT} \quad (22)$$

where

$$L = \int_{T_{PC} - \frac{\Delta T}{2}}^{T_{PC} + \frac{\Delta T}{2}} C_L(T) dT = L \int_{T_{PC} - \frac{\Delta T}{2}}^{T_{PC} + \frac{\Delta T}{2}} \frac{d\alpha_m}{dT} dT \quad (23)$$

Finally, the heat transfer model of the reservoir surface is established, and the energy equation is:

$$\rho C \frac{\partial T}{\partial \tau} = \frac{\partial}{\partial x} \left( \lambda \frac{\partial T}{\partial x} \right) + \frac{\partial}{\partial y} \left( \lambda \frac{\partial T}{\partial y} \right) + \frac{\partial}{\partial z} \left( \lambda \frac{\partial T}{\partial z} \right) \quad (24)$$

According to Figure 2, the analysis of the phase change heat storage reservoir shows that the reservoir is a kind of axisymmetric body. Under these circumstances, the reservoir can be symmetrically simplified. The reservoir is cut along the central axial plane of symmetry, extracting its 1/4 structure as the research area of the numerical simulation. This kind of processing method can ensure the accuracy of the calculation, greatly reduce the demand for computer hardware and the amount of calculation and cost-effectively save the calculation time. The extracted 3D model of the computational region is shown in Figure 3a. The COMSOL Multiphysics software based on the finite element method is used to simulate the above mathematical models and the simulation flowchart is shown in Figure 3b. In order to achieve high computational efficiency, the solver was set as follows: the velocity field was calculated first according to the coupling mass and momentum conservation equations, and then the temperature field was calculated by the velocity distribution previous simulated and energy conservation equations. The PARDISO solver was used to numerically solve the mathematical model established above.

### 3.2. Single-Value Conditions of the Model

#### 3.2.1. Initial Conditions

According to the investigation of underground engineering, the initial temperature of the air-conditioning reservoir in the existing underground engineering in hot summer and cold winter regions is mostly maintained between 18 °C and 21 °C. Therefore, the initial temperature of the simulated reservoir, reservoir surface and phase change heat storage module was set at 19 °C.

#### 3.2.2. Boundary Conditions of Surface

The surface boundary of the reservoir adopts the wall function method, and the surface of the temperature field is the third type of boundary condition:

$$-\lambda \frac{\partial T}{\partial x} \Big|_{surface} = h(T \Big|_{surface} - T_a) \quad (25)$$

where  $h$  is the convective heat transfer coefficient between the outside of the reservoir surface and the air, in  $W/m^2K$ ; and  $T_a$  is the air temperature, in °C.

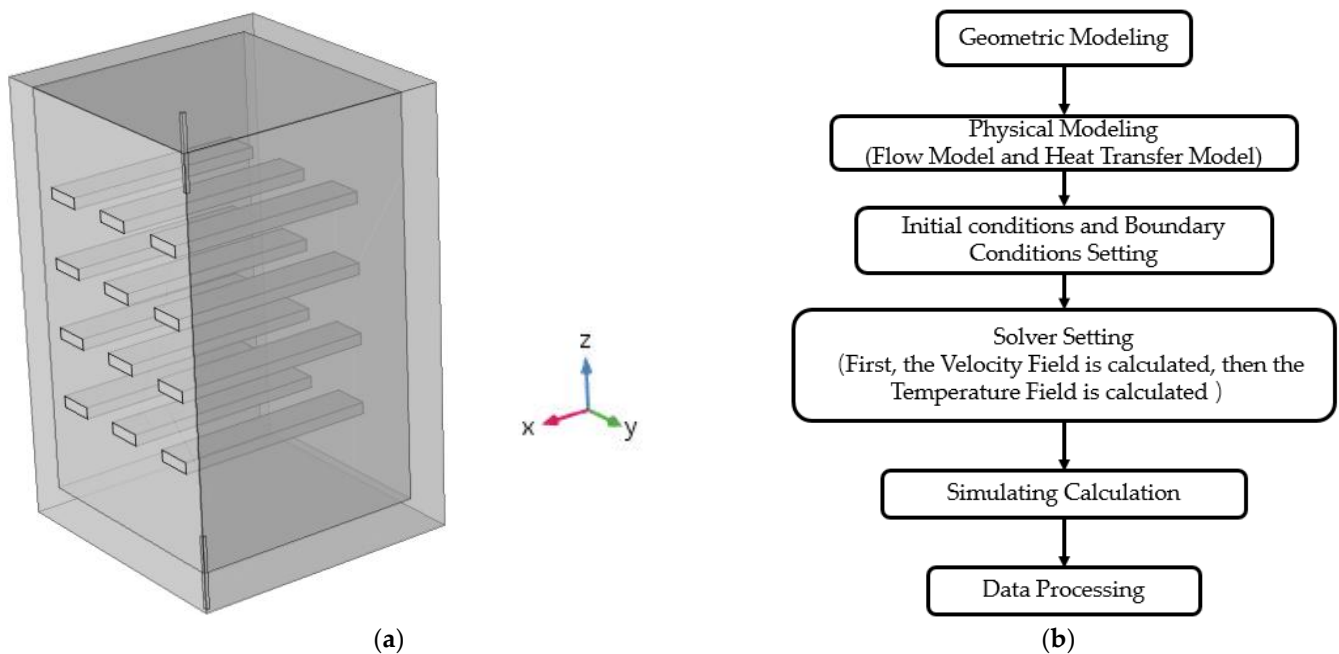


**Figure 3.** Simulation calculation model and simulation process. (a) Simulation calculation model; and (b) Detail simulation flowchart.

### 3.2.3. Boundary Conditions of Inlet and Outlet

The inlet flow boundary conditions adopt a constant velocity boundary. Considering the model established in this research to simulate the working conditions of a constant heating load, the inlet temperature and outlet temperature are coupled, and the expression of inlet temperature is:

$$T_{in} = T_{out} + \frac{q}{C_{pm}} \quad (26)$$

where  $q$  is the heating power of the reservoir, W.

### 3.2.4. Setting of Key Parameters during Simulation of Phase Change Module Model

This research was based on the COMSOL Multiphysics software platform, simulating the heat transfer process of the module of the system using the sensible heat capacity method. The sensible heat capacity method regards the latent heat of the phase change of a substance as having a large sensible heat capacity in a small temperature range. Thus, the phase change process described by partitions is transformed into a nonlinear thermal conduction problem in a single region. The disadvantage of the sensible heat capacity method is that, when the phase change temperature range is very narrow, the equivalent phase change heat conduction process is highly nonlinear and the model convergence is poor. In addition, due to the simulation of unsteady heat transfer under constant heat load, when the time step selected in the simulation is too large, it is easy to cause the temperature rise of PCM at adjacent time to be too large, exceeding the phase change temperature interval set in the model. Under these conditions, it will overheat the stage as it will jump from the solid phase directly to the liquid phase. This will lead to the latent heat being ignored, distorting the calculation results and causing significant differences from the actual situation. To investigate the influence of the time step and phase change temperature interval on the simulation results, several simulation tests were carried out in this research. Considering the calculation accuracy and cost, it is reasonable for the time step to be set at approximately 0.5–2 h and the phase change temperature interval to be set at approximately 2.5 °C.

#### 4. Model Verification

To verify the rationality and correctness of the theoretical model, the heat storage performance test of the reservoir was carried out based on the experimental platform. The PCM-type paraffin produced by Shanghai Joule Wax Industry was selected as the PCM, with models of PCM-1 and PCM-2. Its physical parameters were provided by the manufacturer, as shown in Table 2. The phase change heat storage module was arranged in four layers. The upper two layers discharge the heat storage module encapsulated by phase change wax PCM-2, and the lower two layers discharge the heat storage module encapsulated by phase change wax PCM-1.

**Table 2.** Main physical parameters of PCM-1 and PCM-2 phase change wax.

The Name of the PCM	Melting Point (°C)	Latent Heat (kJ/kg)	Coefficient of Thermal Conductivity (W/m <sup>2</sup> K)	Specific Heat kJ/kg.K
PCM-1 phase change wax	29~30	220	0.21(solid)/ 0.17(liquid)	2.4(solid)/ 3.22(liquid)
PCM-2 phase change wax	31~32	220	0.22(solid)/ 0.17(liquid)	2.6(solid)/ 3.32(liquid)

The temperature of the reservoir and the temperature of the phase change heat storage module are the key points of monitoring during the experiment. A total of eight thermocouple measuring points were arranged in the reservoir, and “#” represents the temperature probe number identifier. Thermocouple 1# was used to monitor the inlet temperature of the reservoir; thermocouples 2#–7# were arranged from top to bottom in the center of the reservoir and vertically at equal distances from the bracket to monitor the vertical temperature of the reservoir; and thermocouple 8# was used to monitor the outlet temperature of the reservoir. A thermocouple probe was arranged at the central point of the module in the middle of each layer to monitor the temperature change of the PCM. The thermocouple temperature data were collected every minute. Figure 4 shows the layout diagram of temperature measuring points of the reservoir and the module under test conditions. The cooling water flow of the reservoir was 350 L/h.

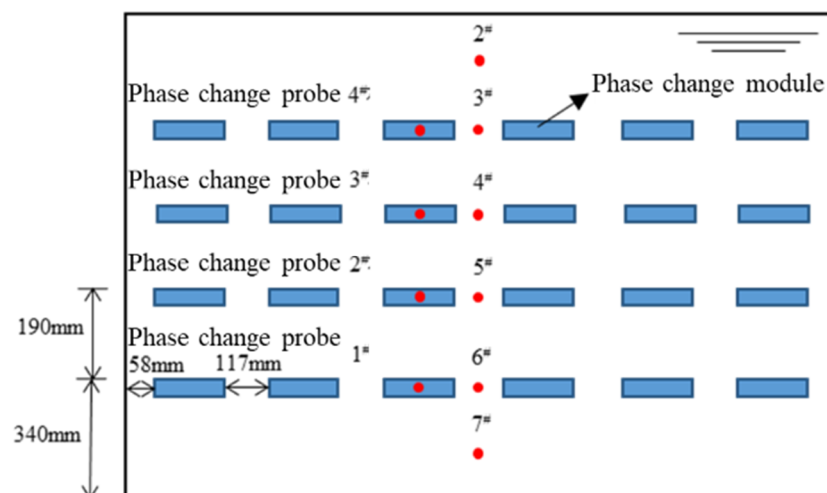


**Figure 4.** Layout diagram of the temperature-measuring points in phase change heat storage reservoir.

The numerical results of the temperature of the inlet and outlet water and the temperature of the phase change module were compared with the experimental results. Figure 5 shows the comparison between the calculated value and the experimental value of the water temperature at the measuring points of the inlet and outlet of the reservoir, and Figure 6 shows the comparison between the calculated value and experimental value of

the internal temperature of the module. The temperature values calculated by the model in this research are in good agreement with the experimental values. This means that the model has a certain accuracy.

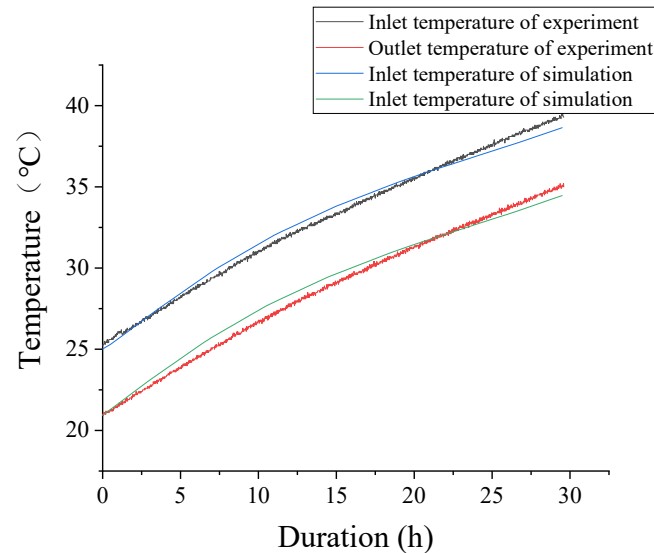


**Figure 5.** Comparison of the experimental and simulated values of temperature during phase change.

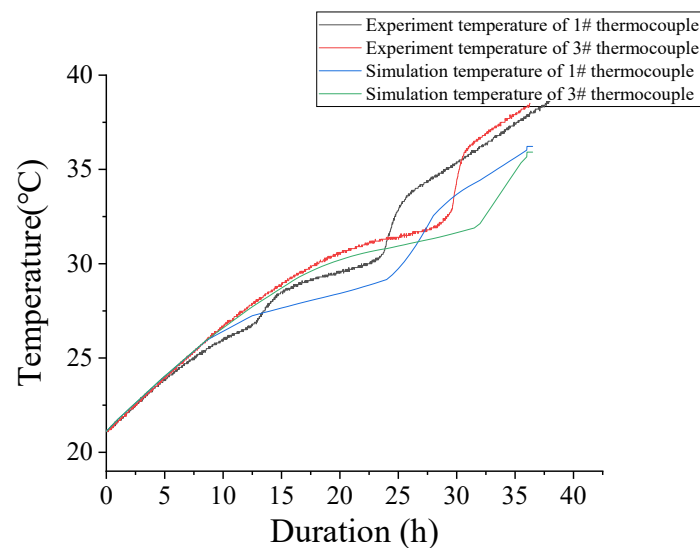


**Figure 6.** Comparison of the experimental and simulated values of internal temperature during phase change heat storage module.

The error between the simulation and experiment can be explained from the following aspects. First, the initial temperature of the material at each point in the device is not the same at the beginning of the test, while the temperature at each point under the initial conditions is uniformly distributed in the numerical calculation. Second, the inlet flow of the cooling water and the heating power of the pipe heater are difficult to keep constant in the actual test process, but these two values are set as constants in the numerical calculation. Third, the physical property parameters of the PCM will change with temperature during the actual test process, but the physical property settings of the PCM are simplified in numerical calculation. Fourth, the boundary conditions are simplified in the numerical calculation, and differ from the actual test conditions. Additionally, compared with the simulation calculation, the amount of encapsulated PCM is insufficient. Due to the difference between the solid and liquid density of the PCM, the volume of test liquid decreases after

encapsulation and solidification. The phase change module is not filled and contains air. In addition, it was found that there was a leakage at the seal during the test, and the amount of paraffin encapsulated in the phase change module was reduced to a certain extent.

In the simulation process, the above experimental effects were not considered. The simulation assumes that the paraffin in the solid phase and liquid phase is completely filled with PCMs, and there is no other material such as air in the phase change modules. The above assumptions will cause the difference in thermal conductivity and filling quantity in both the test and simulation process. In the simulation process, the PCM module has excessive PCM filling and the thermal conductivity is higher. This results in the simulated inlet and outlet water temperature values being lower than the test value in the late simulation. In that case, the simulated heat storage performance of the reservoir is better than the test, and the guaranteed operation time is longer. Due to the small amount and uncertainty of the permeability and complex influence of air infiltration in the packaging process on the heat transfer process, it was not considered under the subsequent simulation conditions. Therefore, the effect of the simulation test may be better than the experimental value. Considering the above experimental errors and the complexity of the phase change heat transfer, the errors between the simulation and experiment are in an acceptable range. Therefore, it can be concluded that the established model can better reflect the coupled heat transfer characteristics between the PCMs and heat transfer fluid of the underground air-conditioning phase change reservoir. Hence, the established mathematical model can be used for the numerical calculation to further analyze the related characteristics of the phase change heat storage reservoir.

### 5. Numerical Simulation Analysis of Heat Storage Performance of Phase Change Reservoir

The heat storage capacity of the phase change reservoir refers to the sensible heat storage capacity and latent heat storage capacity of the water and phase change module. To analyze the heat storage performance of the reservoir in underground engineering, the heat storage capacity per volume and the guaranteed efficiency coefficient of the reservoir were proposed in previous research [31] to measure its heat storage performance. The per volume heat storage of the reservoir is:

$$\Delta q = \frac{\Delta Q}{V} = \frac{mC_w \int_0^{\tau} (t_{in} - t_{out}) d\tau}{V} \quad (27)$$

where  $\Delta q$  refers to the heat storage capacity per volume of the reservoir, in  $\text{kJ}/\text{m}^3$ ;  $V$  refers to the effective heat storage volume of the reservoir, in  $\text{m}^3$ , and its value is  $1.86 \text{ m}^3$  under experimental conditions;  $C_w$  refers to the specific heat capacity of water, in  $\text{kJ}/\text{kg}\cdot\text{K}$ ;  $m$  refers to the cooling water flow of the reservoir, in  $\text{kg}/\text{s}$ ;  $t_{in}$  refers to the inlet temperature of the cooling water of the reservoir, in  $^{\circ}\text{C}$ ;  $t_{out}$  refers to the cooling water outlet temperature of the reservoir, in  $^{\circ}\text{C}$ .

The guaranteed efficiency coefficient of the phase change reservoir defined based on outlet temperature is:

$$\eta = \frac{\tau_p}{\tau_0} \quad (28)$$

where  $\eta$  is the guaranteed efficiency coefficient of the reservoir;  $\tau_p$  is the duration from the initial temperature  $t_0$  to the upper limit of the operating temperature  $t_{lim}$  of the air-conditioning system when the phase change heat storage module is added to the air-conditioning reservoir, in h;  $\tau_0$  is the duration from the initial temperature  $t_0$  to the upper limit of the operating temperature  $t_{lim}$  of the air-conditioning system when no phase change heat storage module is added to the reservoir, in h.

According to the evaluation indexes of the heat storage performance in the underground engineering phase change reservoir proposed above, and taking the phase change heat storage pool system and phase change heat storage module as the research object, the numerical model was established based on the COMSOL Multiphysics software platform. The effects of the PCM properties, the structure size of the phase change heat storage

module and water distribution mode on the operation, performance and efficiency of phase change heat storage system in underground engineering were analyzed.

### 5.1. Influence of Physical Properties of PCMs on Heat Storage Performance of Water Reservoir

Among the physical properties of PCM, the phase change temperature, latent heat value and thermal conductivity of PCM undoubtedly have the greatest influence on the heat storage performance of the system. The influences of these three factors on the heat storage of the system are analyzed in detail below. Table 3 shows the analysis conditions of the influence of the properties of PCMs. To analyze the influence of these three different physical parameters on the heat storage performance of the reservoir, the physical properties of the different materials selected in the numerical calculation are shown in Table 3, and can be divided into three working conditions representing the change in phase change temperature, latent heat value and thermal conductivity, respectively.

**Table 3.** Physical properties of different PCMs.

The Groups	Melting Point (°C)	Latent Heat (kJ/kg)	Coefficient of Thermal Conductivity (W/m·K)
The basic parameters	29	200	0.5
The first group	23 to 33, $\Delta T = 2$	200	0.5
The second group	29	100–250, $\Delta L = 50$	0.5
The third group	29	200	0.2–1.1, $\Delta = 0.3$

#### 5.1.1. Influence of Phase Change Temperature Value of PCM on Heat Storage Performance of Water Reservoir

The phase change temperature of PCMs should be compatible with the system's operating conditions. The temperature of the reservoir's cooling water operation interval is between 21 °C and 35 °C. Considering the fact that PCMs can achieve a phase change to store energy, there must be a temperature gap between the cooling water and the phase change heat storage module for a heat transfer. In that case, the temperature suitable for underground engineering of the phase change temperature range of PCMs should be 21 °C <  $t_m$  < 35 °C.

Taking  $\Delta T = 2$ , the heat storage of the reservoir in underground engineering with a phase change temperature between 21 °C and 33 °C is analyzed. Figure 7 shows the influence of different phase change temperatures on the outlet temperature of the reservoir. As evident in Figure 7, the variation in the outlet water temperature of the reservoir presents three stages.

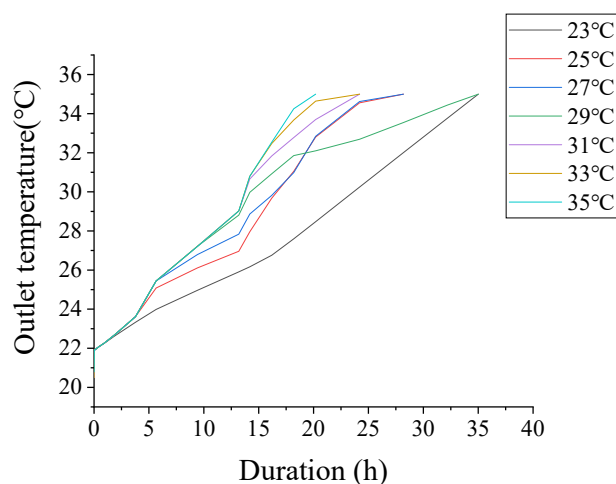


**Figure 7.** Influence of the phase change temperature on the outlet temperature of the reservoir.

The first stage is the heat storage stage dominated by sensible heat. At this stage, because the cooling water of the reservoir and the temperature difference between the phase change heat storage module is small, the phase change heat storage module's internal temperature is below the melting temperature of PCMs. At this time, the condensing heat which was brought into the cooling reservoir is stored in the form of the sensible heat of cooling water and the phase change heat storage module. The outlet temperature of the first stage has a higher slope and faster temperature rise compared with that of the second stage. In the second stage, as the heat storage progresses, the temperature of the module gradually increases. When it reaches the melting temperature of the PCM, latent heat storage begins to play a role in the melting of the PCM. The slope of the exit temperature rise curve at the second stage is significantly lower than that of the first stage. Finally, in the third stage, as the PCM is melted, the heat is again stored in the form of the sensible heat of the cooling water and phase change heat storage module. The slope of the outlet temperature rise curve rises again until the outlet temperature reaches the upper limit of the system's operating temperature. This can also be seen in Figure 7 that with the increase of the melting temperature of the PCM, the outlet temperature begins to rise in the second stage, that is, the initial time of phase change heat storage in the phase change modules is gradually delayed.

Figure 8 shows the analysis of the influence of the phase change temperature on the guaranteed operation time of the reservoir. The analysis shows that, when using the material whose phase change temperature is 33 °C, the guaranteed operation time is significantly less than that of other working conditions. Combined with the change in liquid phase ratio of the phase change module in Figure 9, it can be seen that the reason for this phenomenon is that when the outlet temperature of the heat storage reservoir reaches the upper limit operation temperature  $t_{lim}$ , the module whose phase change temperature is 33 °C has not completely melted and its liquid phase ratio is 46.5%. The heat storage reservoir with PCMs at phase change temperatures of 23 °C, 25 °C, 27 °C, 29 °C and 31 °C completely melted before the outlet temperature reaches the  $t_{lim}$ . The latent heat of the phase change has been fully utilized. There is little difference between the guaranteed operation capacities of the reservoir with phase change temperatures 23 °C and 31 °C. Considering that there was a temperature difference of 2 °C between 31 °C and 33 °C, the phase change temperature was set as 32 °C for the simulation study. The calculated guaranteed operation time is 31.5 h. When the outlet temperature of the reservoir reaches  $t_{lim}$ , the liquid phase ratio is 60.88%. The PCM with the phase change temperature of 32 °C does not complete the phase change when the outlet temperature of the heat storage reservoir reaches  $t_{lim}$ . The latent heat of the phase change is not fully released, thus reducing its guaranteed capacity.

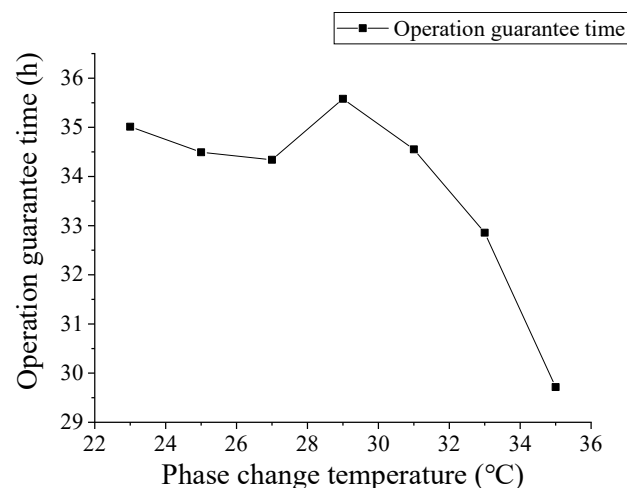
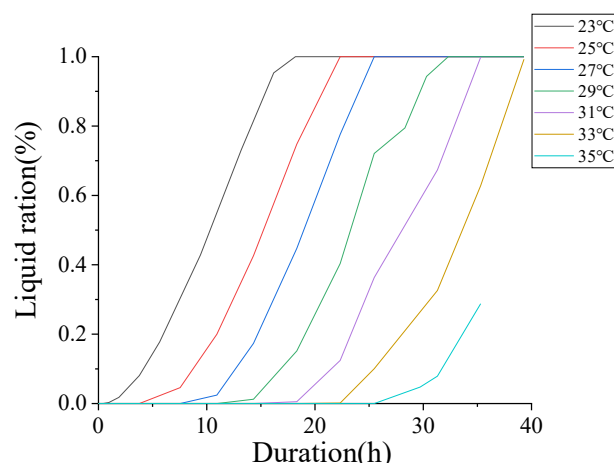


Figure 8. Effect of phase change temperature on the guaranteed operation time of the reservoir.



**Figure 9.** Effect of phase change temperature on melting rate of the heat storage module.

It can be seen from the above analysis that, under the simulated working conditions, the phase change temperature of the selected material should be more than 4 °C lower than the upper limit of the outlet temperature, which ensures that the PCM can be completely melted and the latent heat can be fully released before the outlet temperature of the reservoir reaches  $t_{lim}$  (35 °C).

Further analysis shows that the lower the melting temperature of PCM is, the earlier the phase change heat storage module starts the phase change and completes the heat storage. This seems to be favorable for heat storage. However, combined with the analysis of the heat discharge process of the reservoir, the lower the phase change temperature is, the lower the temperature of the external heat transfer medium required by the solidification and heat release is. When the temperature of the external heat transfer medium is higher, a large amount of phase change stored heat cannot be released, which will inevitably affect the recycling efficiency of the reservoir. This should be considered in practical engineering applications.

Table 4 is the analysis of the influence of different phase change temperatures on the heat storage performance of the reservoir, where the working condition “0” is the simulation of the heat storage process of the reservoir without the phase change heat storage module. It can be seen from Table 4 that the phase change temperature selection of PCMs has a great influence on the heat storage performance of the reservoir. When the phase transition temperature is between 21 °C and 35 °C, the heat storage capacity per volume  $\Delta q$  and the guaranteed efficiency coefficient  $\eta$  are both the highest at 29 °C. Only the phase change temperature suitable for the design condition can give full play to the heat storage efficiency. However, under working condition 6, due to the excessively high phase change temperature, the melt rate of the PCM is low within the variation range of the system-designed operating temperature. This results in its heat storage capacity per volume  $\Delta q$  and the guaranteed heat storage efficiency coefficient  $\eta$  being significantly lower than other conditions.

**Table 4.** Effect of phase change temperature on the performance of the reservoir.

Working Condition	Phase Change Temperature (°C)	$\Delta Q$ (MJ)	$\Delta q$ (MJ/m <sup>3</sup> )	Operation Guarantee Time (h)	$\eta$
0	-	169.13	90.93	26.65	1
1	23	201.81	108.50	31.8	1.19
2	25	203.33	109.32	32.04	1.2
3	27	203.59	109.45	32.08	1.2
4	29	206.31	110.92	32.51	1.22
5	31	203.08	109.18	32	1.2
6	33	195.46	105.09	30.8	1.16

### 5.1.2. Influence of Latent Heat Value of PCM on Heat Storage Performance of Water Reservoir

Considering that the latent heat value of the phase change of existing low-temperature PCMs is mostly between 100 kJ/kg and 250 kJ/kg [34,35], take  $\Delta L = 50$  kJ/kg. The heat storage of the phase change reservoir in underground engineering is analyzed under that condition. Figure 10 shows the influence of different latent heat values of phase change on the outlet temperature of the reservoir.

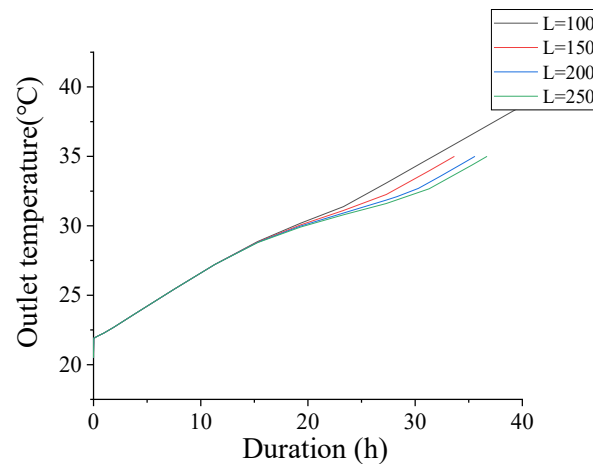


**Figure 10.** Effect of latent heat on the outlet temperature of the reservoir.

Combining Figures 7 and 10, it can be seen that similar to the influence of different phase transition temperatures on the outlet temperature of the reservoir, The outlet temperature of the reservoir under different latent heat values also presents three stages: the first stage of heat storage is dominated by sensible heat; the second stage of heat storage is dominated by latent heat from the changing phase; and the third stage of heat storage is dominated by sensible heat. The slope change stage of the temperature rise curve is the same.

The difference is that the outlet temperature rise and the slope of the reservoir at the first stage are the same under different latent heat values. The reason is that the first stage is the sensible heat storage stage. Apart from the latent heat value of the phase change, all phase change heat storage modules have the same physical parameters.

Further analysis shows that, in the second stage of latent heat storage, with the increase in the latent heat value of the phase change, the outlet temperature of the reservoir presents two significant changes: one is that the slope of the temperature rise curve of the outlet temperature decreases, and the other is that the duration of the phase change heat storage phase increases. The reason for the first phenomenon is that the latent heat value of the phase change increases, which increases the heat storage of PCMs. Nevertheless, the condensing of the heat load into the reservoir is constant, so the heat storage of the water body in the reservoir decreases and the temperature of the water body slowly rises. The reason for the second phenomenon can be seen in Figure 11. The PCMs with different latent heat values have the same phase change temperature, so they all being the phase change at the same moment. The higher the latent heat value of phase change is, then the more the phase change time is delayed, and the longer the time required to complete phase change is. Thus, the duration of the phase change heat storage stage of the reservoir is longer.

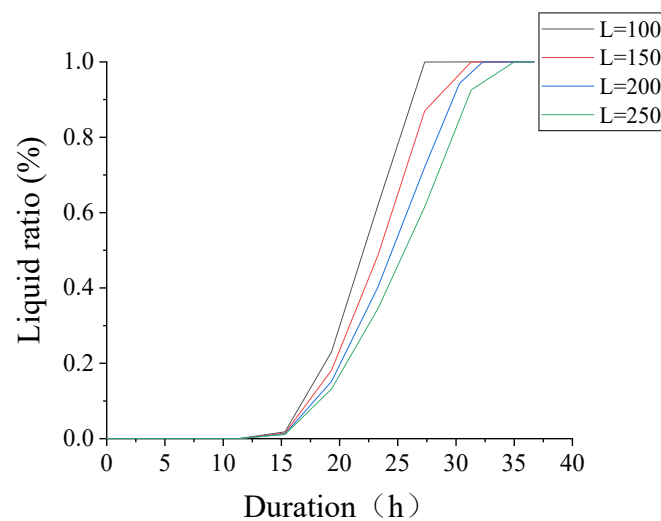


**Figure 11.** Effect of latent heat on the melting rate of the heat storage module.

By analyzing the outlet temperature of the reservoir at the third stage, with the increase in the latent heat value of the phase change, the time required for the outlet temperature to reach the set limit temperature  $t_{lim}$  gradually increases. The main reason is that, as the latent heat value of the phase change increases, the heat storage capacity of the reservoir is enhanced. In that case, it can guarantee the improvement in the operation time of the air-conditioning unit. Therefore, the higher the latent heat value of the phase change is, the more favorable it is to the system energy storage. PCM with high latent heat should be selected as far as possible in the heat storage system of the reservoir.

Figure 12 shows the guaranteed reservoir operation time under different latent heat values of phase change which increases with the increase in the latent heat value. Further analysis shows that, under simulated conditions, the slope increases more when the latent heat value increases from 100 kJ/kg to 200 kJ/kg than when the latent heat value increases from 200 kJ/kg to 250 kJ/kg. That is, with the further increase in the latent heat value, its influence on the guaranteed operation time of the reservoir decreases. In consideration of the reparability and economy of PCM with a high latent heat value, the availability and price of PCM should also be considered in practical engineering design. In a practical application, the PCM with a latent heat value of 200 kJ/kg has more types and a wider selection range than PCM with a latent heat value of 250 kJ/kg.

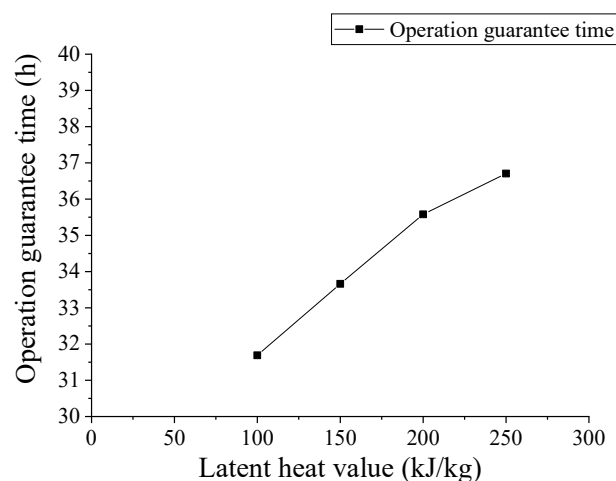


**Figure 12.** Effect of the latent heat value on the guaranteed operation time of the reservoir.

Table 5 shows the analysis of the influence of different latent heat values on the heat storage performance of the reservoir, wherein the working condition “0” refers to the heat

storage process without a phase change heat storage module. As can be seen in Table 5, the latent heat value of the PCM has great influence on the heat storage performance of the reservoir. The heat storage capacity per volume  $\Delta q$  and guaranteed heat storage efficiency coefficient  $\eta$  increase with the increase in latent heat value of PCMs.

**Table 5.** Effect of the latent heat value on the performance of the reservoir.

Working Condition	Latent Heat Value of Phase Transition (kJ/kg)	$\Delta Q$ (MJ)	$\Delta q$ (MJ/m <sup>3</sup> )	Guaranteed Operation Time (h)	$\eta$
0	0	169.13	90.93	26.65	1
1	100	190.39	102.36	30	1.13
2	150	198.64	106.79	31.3	1.17
3	200	206.31	110.92	32.51	1.22
4	250	209.87	112.83	33.07	1.24

### 5.1.3. Influence of Thermal Conductivity of PCMs on Heat Storage Performance of the Reservoir

The value  $\Delta\lambda = 0.3$  is taken to analyze the influence of PCMs with thermal conductivity between 0.2 W/m·K and 1.1 W/m·K on the heat storage performance of the reservoir in underground engineering.

Figure 13 shows the influence of different thermal conductivity values on the outlet temperature of the reservoir. In Figures 10 and 13, it can be seen that under the working conditions of different thermal conductivity values, the temperature change at the outlet of the reservoir generally presents three stages: the first stage of heat storage is dominated by sensible heat; the second stage of heat storage is dominated by latent heat; and the third stage of heat storage is dominated by sensible heat. The slope change at each stage of the temperature rise curve is the same as the previous.

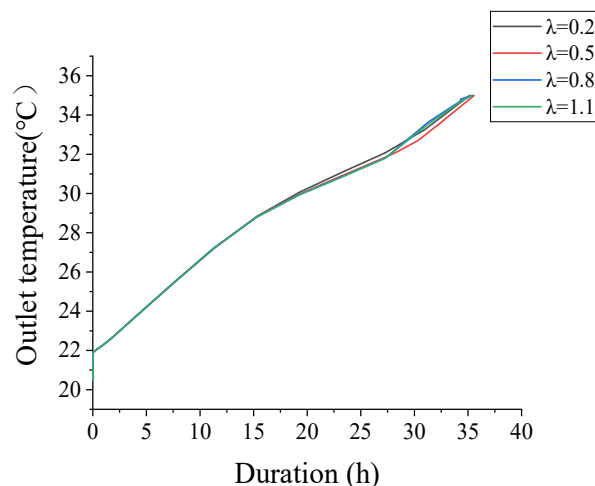
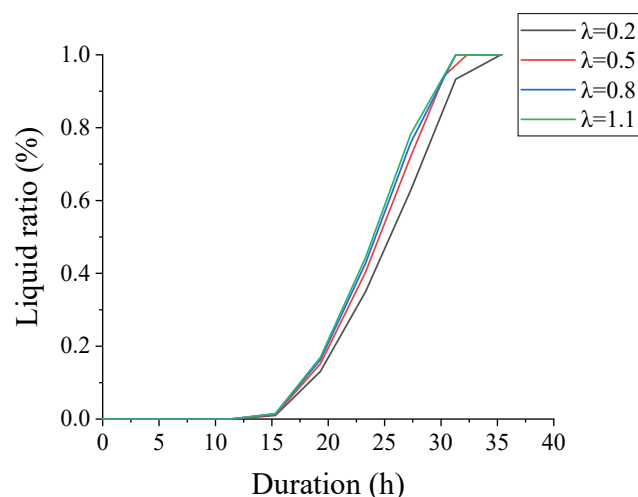


**Figure 13.** Effect of thermal conductivity on the outlet temperature of the reservoir.

It can be seen from Figure 13 that the thermal conductivity has no obvious effect on the outlet temperature of the reservoir, and the four curves almost coincide. However, in the phase change heat storage stage, when the thermal conductivity is 0.2 W/m·K, the slope of the temperature rise in the second stage is higher than under other conditions. The duration of the second stage is longer than under other conditions. The reason is that, when the thermal conductivity value is lower, the melting rate of PCM is slower and the melting duration is longer. As can be seen from the previous analysis, the outlet temperature of the reservoir is significantly affected by the latent heat value and phase change temperature value of the PCM. The influence of thermal conductivity on the heat storage performance of the reservoir is the same under four working conditions in this section. Under the same

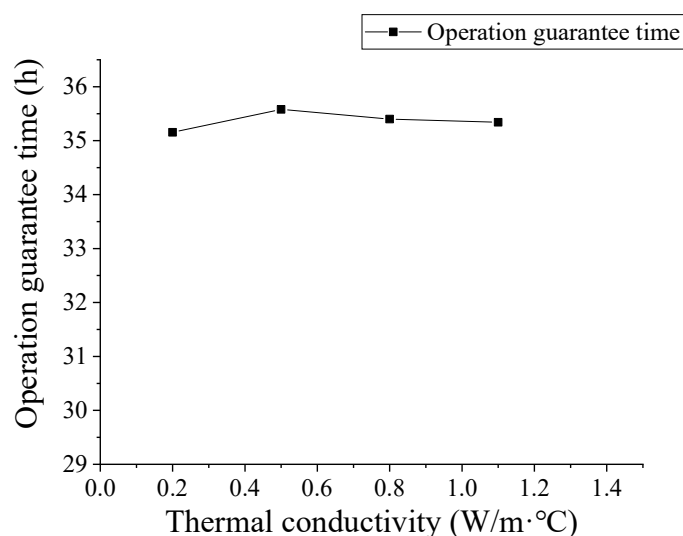
latent heat value and phase change temperature, changing the thermal conductivity of PCM has little influence on the outlet temperature.

Figure 14 shows the influence of different thermal conductivity on the melting rate of PCMs. As can be seen from Figure 14, the difference in the liquid-phase ratio curves increases as the thermal conductivity value increases from 0.2 W/m·K to 1.1 W/m·K. The higher the thermal conductivity value is, the higher the slope of the liquid-phase ratio curve is. This indicates that the melting rate of the PCM is faster, and the time required to complete the melting is shorter. The difference in the curves gradually decreases when  $\lambda > 0.5$  W/m·K. The two liquid-phase curves with thermal conductivity values of 0.8 W/m·K and 1.1 W/m·K partially coincide after  $\lambda > 0.5$  W/m·K. This indicates that, when the thermal conductivity value of PCM is low, the effect of improving the thermal conductivity to enhance the performance of the system is more obvious. When the thermal conductivity of the PCM increases to a certain extent, further increasing the thermal conductivity value will not have a significant effect on the phase change. The thermal conductivity value of PCMs in practical applications is generally very low, such as the use of paraffin wax in this study. According to the above analysis, the thermal conductivity of PCMs must be improved to make the phase change heat storage system run efficiently.



**Figure 14.** Effect of thermal conductivity on the melting rate of PCMs.

Figure 15 shows the influence of different thermal conductivity values on the guaranteed operation time of the reservoir. As can be seen from Figure 15, the guaranteed operation time of the reservoir is the same with different thermal conductivities. This indicates that the thermal conductivity has no obvious influence on the total heat storage of the reservoir. However, increasing the thermal conductivity value can increase the melting rate of PCMs. In that case, it is feasible to enhance the heat transfer and can be considered in practical application. Under experimental conditions, when  $\lambda$  is 0.5 W/m·K, its thermal conductivity has little difference from that when its value is 0.8 W/m·K and 1.1 W/m·K. Compared with the high thermal conductivity value, it is easier to add graphite and other materials into the PCM to increase the thermal conductivity to 0.5 W/m·K. The heat storage of the system will change little due to the addition of fewer other substances. This can also avoid the possibility of reducing the heat storage capacity of the device when too many high thermal conductivity materials are added to the pure PCM.



**Figure 15.** Effect of thermal conductivity on the guaranteed operation time of the reservoir.

Table 6 shows the analysis of the influence of different thermal conductivities on the heat storage performance of the reservoir, in which working condition “0” refers to the heat storage process of the reservoir without the phase change heat storage module. It can be seen from Table 6 that the heat storage capacity per volume  $\Delta q$  and guaranteed heat storage efficiency coefficients  $\eta$  of the reservoirs with different thermal conductivity are the same. This means that the thermal conductivity value of PCM has little influence on the heat storage performance of the reservoir.

**Table 6.** Effect of thermal conductivity on the performance of the reservoir.

Working Conditions	Thermal Conductivity (W/m·K)	$\Delta Q$ (MJ)	$\Delta q$ (MJ/m <sup>3</sup> )	Guaranteed Operation Time (h)	$\eta$
0	0.5	169.13	90.93	26.65	1
1	0.2	205.49	110.48	32.38	1.22
2	0.5	206.31	110.92	32.51	1.22
3	0.8	206.38	110.96	32.52	1.22
4	1.1	206.25	110.89	32.50	1.22

### 5.2. Influence of the Geometric Size of Phase Change Heat Storage Module on Heat Storage Performance of the Reservoir

On the premise of not changing the effective volume of the phase change heat storage module, which also refers to the content of PCMs in the module, the geometric size of the phase change heat storage module is changed to analyze the influence of the structural size of the module on the heat storage performance of the reservoir and the module. The geometric size simulation schemes of the phase change heat storage module are designed, as shown in Table 7.

**Table 7.** Geometric size simulation scheme of the phase change heat storage module.

Scheme	Geometric Type of Section	Section Size (mm)
1	A rectangle	100 × 30
2	A rectangle	30 × 100
3	A rectangle	150 × 20
4	A rectangle	20 × 150
5	A rectangle	75 × 40
6	A rectangle	40 × 75
7	A square	57.44 × 57.44

The heat storage process of the reservoir with different shapes of the modules was numerically simulated, and the influence of the shape on the heat storage performance of the reservoir was compared and analyzed. The aim was to determine the reasonable packaging and layout of PCMs. In each scheme, only the section size of the module was changed, and the length remains unchanged. The physical properties of PCMs are shown in Table 3.

Figure 16 shows the influence of geometric dimensions of the phase change heat storage module on the outlet temperature of the reservoir. It can be seen from Figure 16 that different geometric dimensions of the modules have a certain influence on the outlet temperature of the reservoir. Figure 17 shows the simulated influence of the geometric dimensions of the module on the operation guaranteed time of the reservoir. According to the simulation calculation results, the order of a guaranteed operation time from long to short is: 75 mm × 40 mm, 30 mm × 100 mm, 150 mm × 20 mm, 57.44 mm × 57.44 mm, 20 mm × 150 mm, 40 mm × 75 mm and 100 mm × 30 mm.

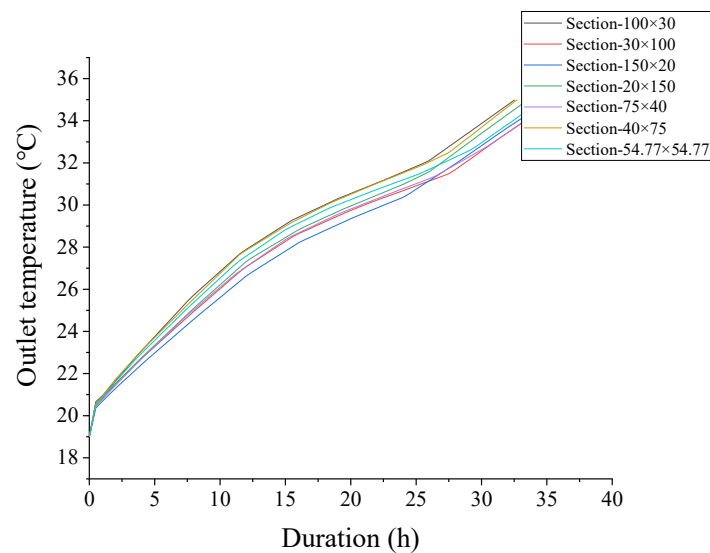


**Figure 16.** Effect of the geometric size of phase change heat storage module on the outlet temperature of the reservoir.

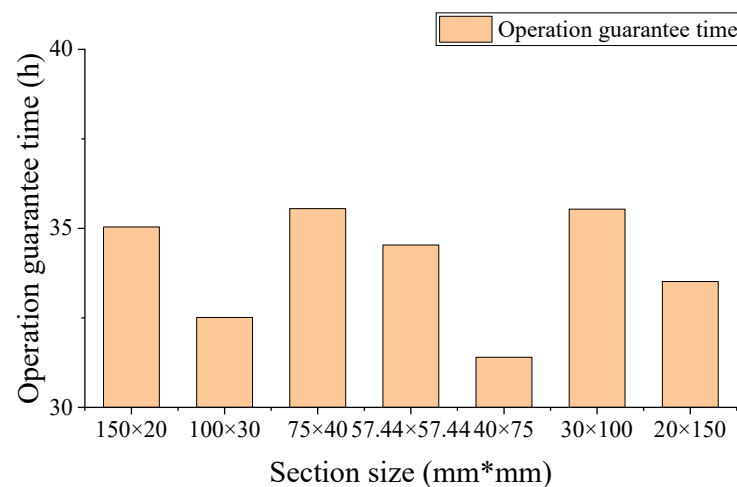


**Figure 17.** The influence of phase change heat storage module geometry size on the guaranteed operation time of the reservoir.

Further analysis of the numerical model shows that the calculation grid needs to be redivided every time the geometric size of the module is changed. This is different

from studying the change in the physical properties of PCMs. At the same time, affected by the step size of the simulation calculation, even though the external heating power input by the model is the same, there are still some calculation errors between working conditions, which are reflected in certain errors in the heat storage calculated by the water body, reservoir surface and phase change heat storage module. This will result in different calculated heat storage power. The calculated heat storage and calculated heat storage power values corresponding to the geometric dimensions of different phase change heat storage modules are shown in Table 8. The results in the table are the values obtained by simulating the 40 h duration.

**Table 8.** Calculated heat storage and calculated heat storage power corresponding to geometric sizes of different phase change heat storage modules.

Scheme	Section Size (mm)	Calculated Heat Storage (MJ)	Calculated Heat Storage Power (kW)
1	100 × 30	251.42	1.746
2	30 × 100	239.47	1.663
3	150 × 20	243.94	1.694
4	20 × 150	251.42	1.746
5	75 × 40	238.03	1.653
6	40 × 75	261.65	1.817
7	57.44 × 57.44	244.66	1.699

As shown in Table 8, the heat storage power obtained by simulation calculation has certain errors under different conditions of the phase change heat storage module size. When the cross-section size change has little influence on the inlet and outlet water temperature, the difference in the guaranteed system operation time caused by this error may be greater than the change caused by actual different sizes. For example, in the numerical calculation, the guaranteed operation time is the longest when the section size of the module is 75 mm × 40 mm. However, Table 8 shows that its calculated heat storage power is the lowest. As such, the influence of the section size on the guaranteed operation time cannot be scientifically evaluated. Therefore, when the calculated heat storage power is different, it is not advisable to judge the influence of the change of the module's section size on the operation effect of the system based on the guaranteed operation time.

To avoid the effect of different calculated heat storage quantities of the reservoir on the efficiency, an improvement indicator appears to evaluate the heat storage performance of the underground air-conditioning reservoir. This indicator is  $\varepsilon$ , which refers to the slope of the temperature rise per unit load of the reservoir. It is defined as the ratio between the slope of the outlet temperature change with time and the heat storage power after the phase change heat storage reservoir runs for a period of time. Its calculation formula is:

$$\varepsilon = \frac{[t_{in}(\tau) - t_0]/\tau}{q} \quad (29)$$

where  $\varepsilon$  is the slope of temperature rise per unit load of heat storage reservoir; and  $q$  is calculated heat storage power, kW.

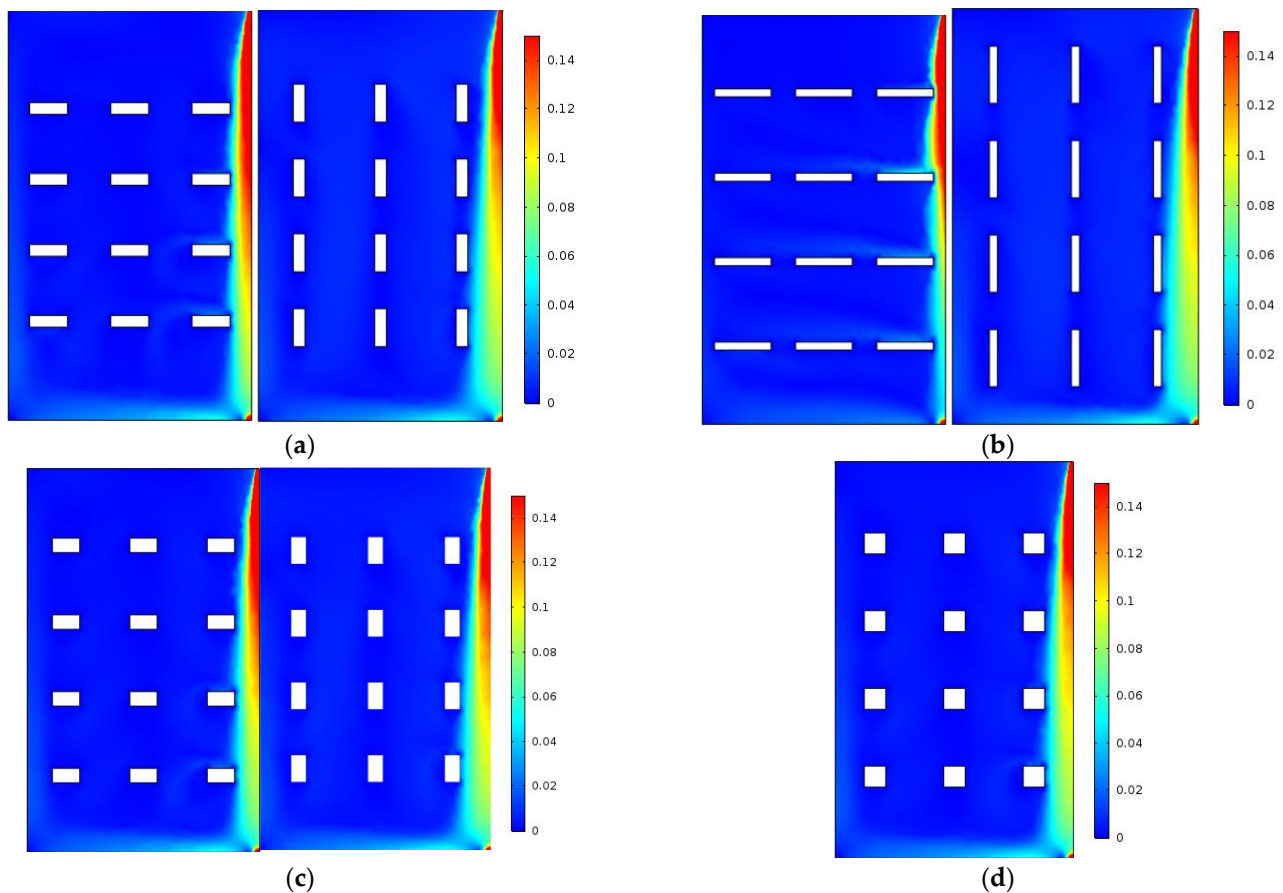
In the same heating time, the lower the slope  $\varepsilon$  of temperature rise per unit load of the reservoir is, the slower the temperature rise at the outlet of the reservoir is, the longer it takes to reach the upper temperature of system operation and the stronger the guaranteed capacity of the reservoir is.

Table 9 shows the slope of temperature rise per unit load of reservoir corresponding to the geometric dimensions of different phase change heat storage modules. As can be seen from Table 9, the slope of the temperature rise per unit load of the reservoir  $\varepsilon$  does not change much under the different geometric dimensions of the module. The results show that the change in the module geometry has no obvious effect on the heat storage performance of the reservoir.

**Table 9.** Temperature increase slope of unit load of reservoir corresponding to geometric sizes of different phase change heat storage modules.

Scheme	Section Size (mm)	Calculated Heat Storage Power (kW)	$\varepsilon$
1	100 × 30	1.746	0.269
2	30 × 100	1.663	0.261
3	150 × 20	1.694	0.259
4	20 × 150	1.746	0.263
5	75 × 40	1.653	0.265
6	40 × 75	1.817	0.263
7	57.44 × 57.44	1.699	0.264

Further analysis shows that the module with a cross-section size of 150 mm × 20 mm has the minimum  $\varepsilon$  value. Figure 18 shows the  $y$ - $z$  section flow field distribution at the inlet center of the reservoir under different sizes of modules. To intuitively display the flow field distribution in the reservoir, the display range of the velocity field cloud map is 0–0.15 m/s, and the actual inlet flow rate is 0.55 m/s (the same below).



**Figure 18.** Flow field distribution chart of a reservoir under different phase change heat storage module sizes: (a) section size 100 mm × 30 mm, 30 mm × 100 mm; (b) section size 150 mm × 20 mm, 20 mm × 150 mm; (c) section size 75 mm × 40 mm, 40 mm × 75 mm; and (d) section size 57.44 mm × 57.44 mm.

By Figure 18b, section size 150 mm × 20 mm of the module has a more distinct phenomenon that shunts a high-temperature cooling water inflow from the reservoir entrance than other sizes. The water mixing effect is better and the heat exchange area is the largest. Under this section size of 150 mm × 20 mm, the slope value  $\varepsilon$  of the temperature rise

per unit load is smaller than that of other section sizes. In practical engineering applications, the size of the module should increase the heat exchange area as much as possible and promote the full mixing of heat.

5.3. Influence of Water Distribution Mode on Heat Storage Performance of Reservoir

As can be seen from the analysis of the influence of the size of the module on the heat storage performance of the reservoir, the change in the flow field in the reservoir has an impact on it. In this study, the influence of different water distribution modes on the heat storage performance of the reservoir was discussed. Different water distribution schemes were designed for the reservoir, as shown in Table 10.

Table 10. Water Distribution Schemes for the Reservoir.

Scheme	Water Distribution Modes	Scheme	Water Distribution Modes
1	One-inlet-one-outlet	5	Three-inlets-three-outlets-b
2	Two-inlets-two-outlets-a	6	Four-inlets-four-outlets
3	Two-inlets-two-outlets-b	7	Four-inlets-one-outlet
4	Three-inlets-three-outlets-a		

The heat storage process of the reservoir under different water distribution modes was numerically simulated. The influence on the heat storage performance of the reservoir was comparatively analyzed. The aim was to determine the optimal water inlet and outlet layout. The physical properties of PCMs selected in the research are shown in Table 3. A 1/4 model of the reservoir with different water distribution modes is shown in Figure 19.

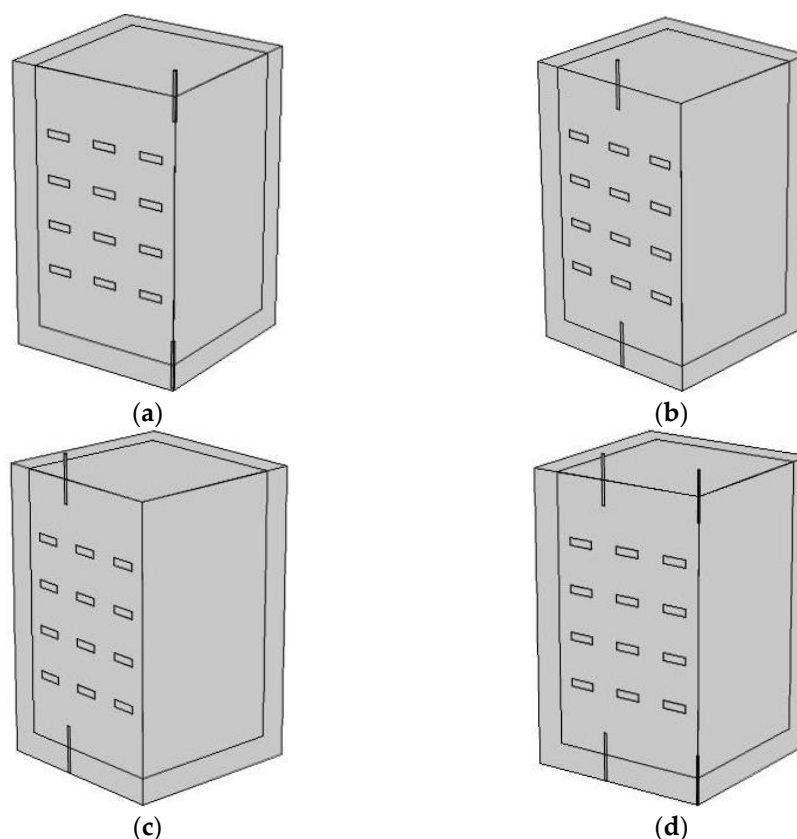
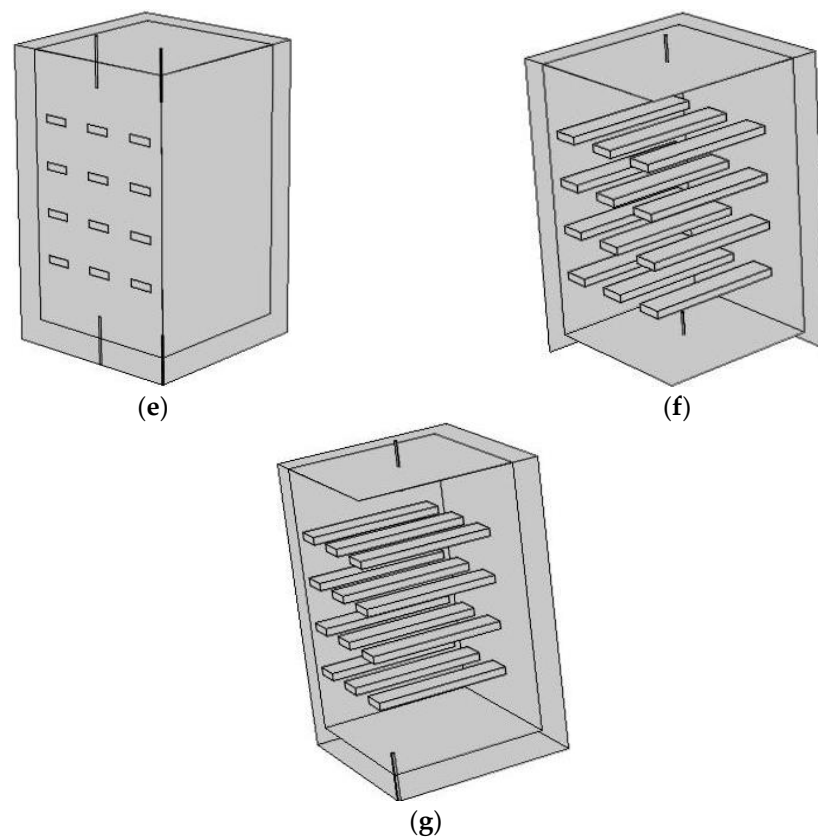
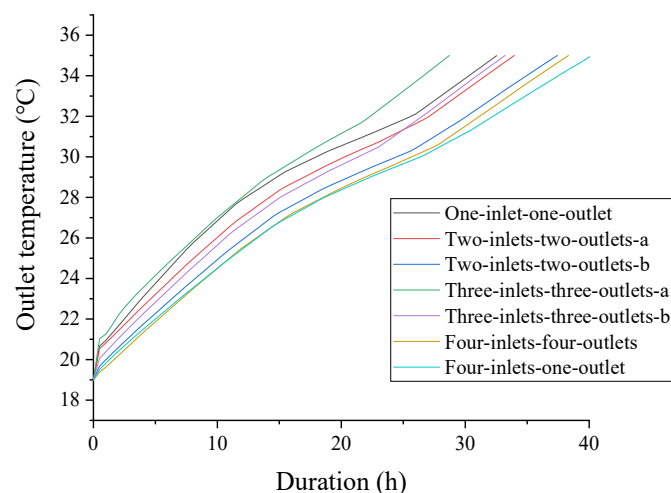


Figure 19. Cont.



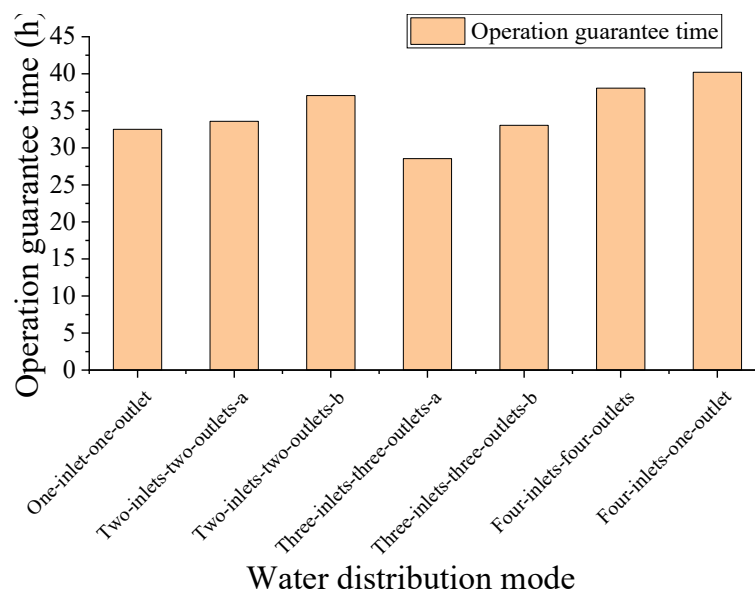
**Figure 19.** Water distribution scheme: (a) one-inlet–one-outlet; (b) two-inlets–two-outlets-a; (c) two-inlets–two-outlets-b; (d) three-inlets–three-outlets; (e) three-inlets–three-outlets-b; (f) four-inlets–four-outlet; and (g) four-inlets–one-outlet.

Figure 20 shows the influence of the water distribution modes on the outlet temperature of the reservoir. It can be seen from Figure 20 that the different water distribution modes have a great influence on the outlet temperature of the reservoir. The analysis shows that, among all water distribution modes, the optimal mode is the four-inlets–one-outlet water distribution mode. Under this circumstance, the duration required for the outlet water temperature to reach the upper operating temperature of the system is 40.2 h. In the case of the three-inlets–three-outlets-a water distribution mode, the duration required for the outlet water temperature to reach the upper operating temperature of the air-conditioning system is 28.7 h, which is the most unfavorable mode.



**Figure 20.** Effect of simulated water distribution on the outlet temperature of the reservoir.

Figure 21 shows the influence of the simulated water distribution modes on a reservoir guaranteed operation time. According to the simulation results, the order of the guaranteed operation times from longest to shortest is four-inlets–one-outlet; four-inlets–four-outlets; two-inlets–two-outlets-b; two-inlets–two-outlets-a; three-inlets–three-outlets-b; one-inlet–one-outlet; and three-inlets–three-outlets-a.



**Figure 21.** The influence of water distribution mode on the guaranteed operation time of reservoir.

Further analysis of the numerical model shows that there are still some calculation errors between the different water distribution modes, which is the same as in the study of the geometric size change of the phase change heat storage module. This refers to the fact that there are errors when calculating the heat storage quantity by the water, the surface and the phase change heat storage module. This leads to the difference in calculating the heat storage power. Different heat storage quantities and their power are calculated by various water distributions, which can be seen in Table 11. The calculated heat storage and e power values of each working condition in the table are the values obtained by simulating for 40 h.

**Table 11.** Calculated heat storage and calculated heat storage power corresponding to different water distribution modes.

Scheme	Water Distribution Modes	Calculated Heat Storage (MJ)	Calculated Heat Storage Power (kW)
1	One-inlet–one-outlet	251.42	1.746
2	Two-inlets–two-outlets-a	249.84	1.735
3	Two-inlets–two-outlets-b	242.78	1.686
4	Three-inlets–three-outlets-a	270.00	1.875
5	Three-inlets–three-outlets-b	261.50	1.816
6	Four-inlets–four-outlets	241.34	1.676
7	Four-inlets–one-outlet	230.26	1.599

As shown in Table 11, under different conditions of water distribution, the heat storage power obtained by the simulation calculation also has certain errors, and the fluctuation range is larger than the error value under the different conditions of the geometric size change of phase transition module. Due to the existence of the error, the conclusion of the influence the water distribution mode on the guaranteed operation time cannot be scientifically drawn. For example, in the above analysis, the four-inlets–one-outlet water distribution mode has the longest guaranteed operation time. Nevertheless, its calculated heat storage power is the lowest according to Table 11. The three-inlets–three-outlets-a

water distribution mode is the most unfavorable, but its calculated heat storage power is the highest. Therefore, when the calculated heat storage power values are different, it is not advisable to judge the influence of water distribution modes according to the guaranteed operation time.

To avoid the influence of different heat storage quantities on the evaluation of the guaranteed capacity of the reservoir, the slope of temperature rise per unit load of the reservoir  $\varepsilon$  was also used as an evaluation index to investigate the influence of the water distribution mode on the system operation.

Table 12 shows the slope of temperature rise per unit load of reservoirs corresponding to different water distribution modes. It can be seen from Table 12 that the slope of temperature rise per unit load  $\varepsilon$  of the reservoir varies greatly under different water distribution modes. This indicates that the change in water distribution mode has an obvious influence on the heat storage performance.

**Table 12.** Temperature increase slope of reservoir unit load corresponding to different water distribution modes.

Scheme	Water Distribution Modes	Calculated Heat Storage Power (kW)	$\varepsilon$
1	One-inlet–one-outlet	1.746	0.269
2	Two-inlets–two-outlets-a	1.735	0.262
3	Two-inlets–two-outlets-b	1.686	0.248
4	Three-inlets–three-outlets-a	1.875	0.275
5	Three-inlets–three-outlets-b	1.816	0.255
6	Four-inlets–four-outlets	1.676	0.244
7	Four-inlets–one-outlet	1.599	0.244

Figures 22 and 23, respectively, show the flow field and temperature distribution of the  $y$ – $z$  section air-conditioning reservoir at the inlet center under different water distribution modes. The analysis shows that the flow field and temperature distribution in the reservoir differ greatly under different water distribution modes. In Figure 22a,b,d, the modes whose temperature rise slope is high are one-inlet–one-outlet, two-inlets–two-outlets-a and three-inlets–three-outlets-a. After the fluid enters the reservoir from the inlet, the water flows downward along the gap of the module. The flow velocity on the inlet and outlet channel of the reservoir is high, and the flow retention area in the reservoir is large. Corresponding to Figure 23a,b,d, the temperature in the inlet and outlet passage of the reservoir is high, and the temperature distribution in the reservoir is not uniform. As a result, when the outlet temperature has reached its limitation, the temperature in most areas of the reservoir has not reached the upper limit of the system, and the heat storage effect of the reservoir is not good. As shown in Figure 23d, especially under the conditions of three-inlets–three-outlets-a, due to the influence of the flow field in this arrangement, there is an obvious thermal short circuit phenomenon between the exits. Heat accumulates at the outlet, causing the outlet temperature to be significantly higher than that of the area outside the inlet and outlet passage. Thus, the slope value of the temperature rise per unit load is large, and the guaranteed operation capacity of the reservoir is poor.

By Figure 22c,e,f, the modes whose temperature rise slope is low are two-inlets–two-outlets-b, three-inlets–three-outlets-b and four-inlets–four-outlets. After the fluid enters the reservoir from the inlet, the water flow scours the phase change heat storage module, and the water flow is strongly disturbed. The flow field in the reservoir is evenly distributed, and no high-speed passage is formed between the inlet and outlet. Corresponding to Figure 23c,e,f, the quantity of heat quickly spreads around. The temperature field in the reservoir is evenly distributed, and there is no obvious temperature difference between the outlet of the reservoir and the surrounding water. This means that the slope value of the temperature rise per unit load is small, and the guaranteed reservoir operation capacity is good.

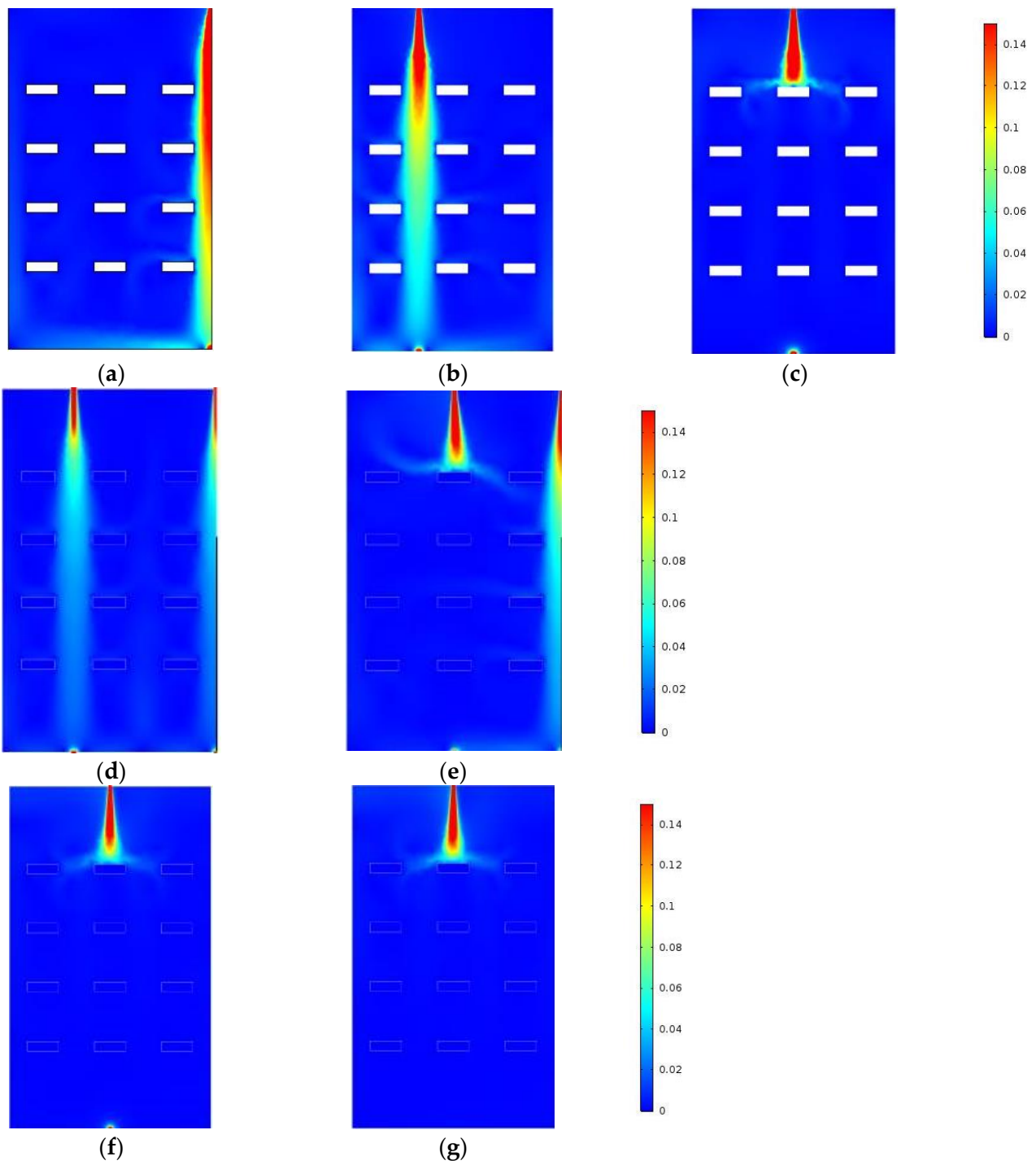


**Figure 22.** Flow field distribution chart of the reservoir under different water distribution modes: (a) one-inlet-one-outlet; (b) two-inlets-two-outlets-a; (c) two-inlets-two-outlets; (d) three-inlets-three-outlets-a; (e) three-inlets-three-outlets-b; (f) four-inlets-four-outlets; and (g) four-inlets-one-outlet.

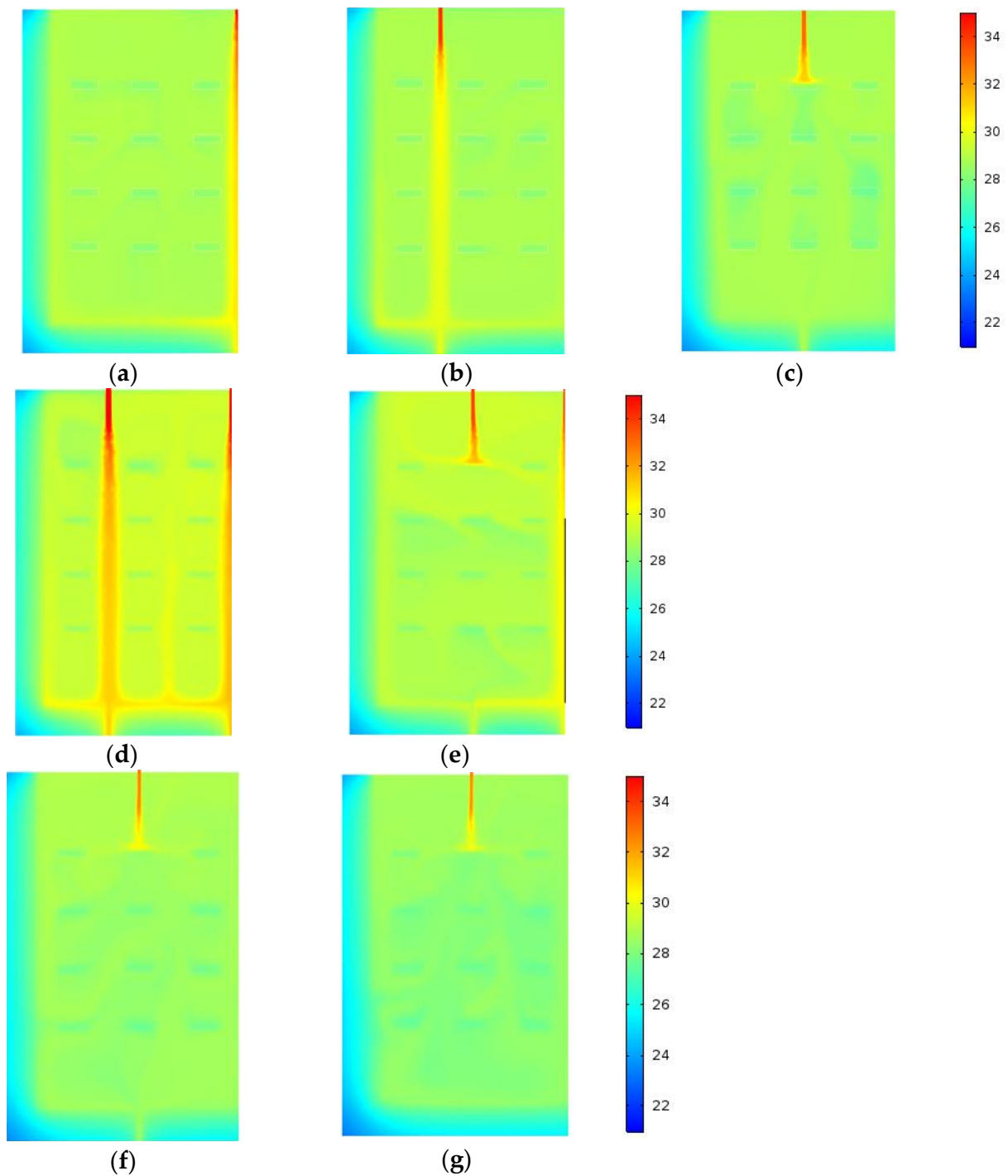


**Figure 23.** Temperature cloud of the reservoir at 20 h under different water distribution modes: (a) one-inlet-one-outlet; (b) two-inlets-two-outlets-a; (c) two-inlets-two-outlets; (d) three-inlets-three-outlets-a; (e) three-inlets-three-outlets-b; (f) four-inlets-four-outlets; and (g) four-inlets-one-outlet.

As shown in Figure 22e, under the distribution of three-inlets-three-outlets-b, the inlet and outlet located in the middle failed to flush the phase change heat storage module. The thermal short circuit still exists in the middle inlet and outlet channel, as shown in Figure 23e. Therefore, with the comparison between two-inlets-two-outlets-b and four-inlets-four-outlets, the slope of the temperature rise per unit load of three-inlets-three-outlets-b is slightly larger, and the reservoir guaranteed operation capacity is slightly poor. Compared with two-inlets-two-outlets-b, the four-inlets-four-outlets water distribution

mode has a more uniform water distribution, larger area of scouring phase change heat storage module, more obvious flow disturbance and more significant heat diffusion. The slope value of temperature rise per unit load is smaller, and the guaranteed reservoir operation capacity is better.

To further investigate the influence of the outlet change on the heat storage performance of the reservoir, four-inlets–four-outlets-and four-inlets–one-outlet were compared. It can be seen from Figure 22f,g that the flow field distribution in the reservoir is consistent. The corresponding temperature field distribution in the reservoir is also basically consistent, as shown in Figure 23f,g. Meanwhile, it can be seen from Table 10 that the slope of temperature rise per unit load  $\varepsilon$  of the reservoir is the same. In the case of the reservoir layout of four inlets, there is no significant difference between the one outlet and four outlets.

To sum up, the water distribution modes of the reservoir show obvious disturbances in the water body, which affect the heat exchange and the overall heat storage effect. Therefore, in the upper-to-lower mode of water distribution, the thermal short circuit between the inlet and outlet should be avoided. The layout position of the phase change heat storage module in the reservoir should be fully utilized to enhance the water flow disturbance so that the inlet water flow can exchange heat with the water in the reservoir as soon as possible. Under the modeling conditions established in this research, it is necessary to make the water flow directly scour the module, instead of arranging the water inlet and outlet towards the gap between them. In addition to the above conditions, the uniform water distribution mode with multiple inlets is more conducive to enhancing the heat storage capacity of the reservoir and improving the guaranteed operation time of the system.

## 6. Conclusions

A three-dimensional unsteady heat transfer numerical model of a phase change reservoir in underground engineering was established in this paper. The influence on the reservoir's heat storage performance of PCM's phase change temperature, latent heat value, thermal conductivity, encapsulation size and the water distribution modes was calculated and analyzed. The heat storage per unit volume of the phase change reservoir and the support efficiency coefficient were defined based on outlet temperature, and the temperature rise slope per unit load of the heat storage reservoir was evaluated. The following conclusions were drawn:

- (1) By studying the influence of the physical parameters of PCMs on the heat storage performance of the reservoir, it was found that: the phase change temperature of the PCM should be less than the upper limit of the reservoir outlet temperature of 4 K. When the phase change temperature was 29 °C, the efficiency coefficients of the heat storage  $\eta$  are 1.22, and heat storage support per unit volume  $\Delta q$  are 110.92 MJ/m<sup>3</sup>, which were the maximum values under various working conditions that the phase change temperature tested increased from 21 °C to 35 °C. This means that the heat storage capacity of the reservoir reaches the best. The heat storage capacity of the PCM reservoir increases with the increase in latent heat in the range of 0~250 kJ/kg. When the latent heat value of PCM is 250 kJ/kg, its heat storage support per unit volume  $\Delta q$  and heat storage efficiency coefficients are  $\eta$  112.83 MJ/m<sup>3</sup> and 1.24, respectively, which are the maximum values under working conditions. The thermal conductivity has little effect on the heat storage performance of PCM when it increases from 0.2 W /m·K to 1.1 W /m·K.
- (2) In this paper, different geometric sections are set, respectively: the phase change heat storage modules of 100 mm × 30 mm, 30 mm × 100 mm, 150 mm × 20 mm, 20 mm × 150 mm, 75 mm × 40 mm, 40 mm × 75 mm and 57.44 mm × 57.44 mm were compared. The slope of the temperature rise per unit load of the heat storage reservoir is 0.269, 0.261, 0.259, 0.263, 0.265, 0.263 and 0.264, respectively. The slope of the temperature rise per unit load of the reservoir with the geometric cross-section size of 150 mm × 20 mm is the lowest, which indicates that under the condition of the same volume of the phase change module, the greater the contact between the module

and water area is, the stronger the degree of transverse scouring by water flow, and the better its comprehensive heat storage performance. Therefore, in the actual design, the heat storage capacity of the phase change module can be further enhanced by improving the conditions of enhanced heat transfer when the heat storage volume of the phase change module is constant.

- (3) Under the modeling conditions established in this paper, seven heat storage reservoir working conditions were set under the overall water distribution modes of water flowing in and out of the heat storage reservoir: one-inlet–one-outlet; two-inlets–two-outlets-a; two-inlets–two-outlets-b; three-inlets–three-outlets-a; three-inlets–three-outlets-b; four-inlets–four-outlets; and four-inlets–one-outlet, for which the slope of the temperature rise per unit load of the reservoir is 0.269, 0.262, 0.248, 0.275, 0.255, 0.244 and 0.244, respectively. Increasing water inlets can improve the heat storage capacity of the reservoir. Further analysis of the influence of water inlets' position on the temperature field and flow field under various working conditions shows that the more the water distribution at water inlets is uniform, the larger the area of scouring phase change heat storage module is, the more obvious the water flow disturbance in the reservoir is, the more uniform the distribution of temperature field and flow field is and the stronger the heat storage capacity is.

**Author Contributions:** Conceptualization, S.L.; formal analysis, H.Z.; investigation, X.S. and Z.S.; methodology, G.H.; project administration, C.Z.; visualization, L.C. and N.X.; writing—original draft, F.G.; writing—review and editing, S.H. All authors have read and agreed to the published version of the manuscript.

**Funding:** This research was funded by “the Science and Technology Research Program of Chongqing Municipal Education Commission grant number Grant No. KJZD-K202112902”; “the Project of Chongqing Natural Science Foundation grant number cst2020jcyj-msxmX0372”; and “Graduate Joint training Base of Army Logistics Academy and Chongqing Midea General Refrigeration Equipment Co., Ltd.” grant number Chongqing Educational Development (2019) no. 12.

**Institutional Review Board Statement:** Not applicable.

**Informed Consent Statement:** Not applicable.

**Data Availability Statement:** Not applicable.

**Conflicts of Interest:** The authors declare no conflict of interest.

## References

- Mao, J.; Li, Y.; Geng, S.; Han, X.; Zhang, H.; Li, W.; Wang, L.; Jiang, J.; Chen, J. Research progress of thermal environment inside protection works. *Heat. Vent. Air Cond.* **2012**, *42*, 6–12.
- Yi, Z. Preliminary study on protection engineering construction and prevention strategy under the condition of information war. *Sci. Technol. Inf.* **2012**, *16*, 451.
- Zhang, Y.; Miao, X.; Peng, F.; Jiang, F.; Yang, J. Research on protection effectiveness evaluation of condensation heat processing systems in protective engineering. *Prot. Eng.* **2016**, *1*, 48–53.
- Wang, J.; Liu, W.; Cai, H.; Yuan, L.; Wang, J. Underground Thermal Storage Defensive Cooling Tower. *Refrig. Air Cond.* **2010**, *24*, 1–3.
- He, Y. *Study on the Indirect Evaporative Cooler for Metro*; Chongqing University: Chongqing, China, 2009.
- Liu, Y.; Wang, S.; Jin, Y.; Wang, T. Discussion on the location of cooling tower in protective engineering. *Prot. Eng.* **2012**, *1*, 64–67.
- Geng, S.B.; Li, Y.; Han, X.; Liu, Y.H.; Guo, X.S. Water loop heat pump system in underground engineering. *J. PLA Univ. Sci. Technol. Nat. Sci. Ed.* **2011**, *12*, 139–143.
- Zhang, H.; Mao, J.; Li, Y. Research of Ground Source Dehumidifying & Air-condition System in Civil Engineering. *Refrig. Air Cond.* **2010**, *24*, 30–34.
- Wang, J.; Mao, J.; Han, X.; Li, Y. Study on analytical solution model of heat transfer of ground heat exchanger in the protection engineering structure. *Renew. Energy* **2021**, *179*, 998–1008. [[CrossRef](#)]
- Chen, F.; Mao, J.; Zhu, G.; Zhang, B.; Tian, Y.; Liao, D.; Liu, Y. Numerical assessment on the thermal imbalance of multiple ground heat exchangers connected in parallel. *Geothermics* **2021**, *96*, 102191. [[CrossRef](#)]
- Chen, F.; Mao, J.; Chen, S.; Li, C.; Hou, P.; Liao, L. Efficiency analysis of utilizing phase change materials as a grout for a vertical U-tube heat exchanger coupled ground source heat pump system. *Appl. Therm. Eng.* **2018**, *130*, 698–709. [[CrossRef](#)]

12. Meng, Z.N.; Zhang, P. Experimental and numerical investigation of a tube-in-tank latent thermal energy storage unit using composite. *PCM Appl. Energy* **2017**, *190*, 524–539.
13. Xu, C.; Zhang, H.; Fang, G. Review on thermal conductivity improvement of phase change materials with enhanced additives for thermal energy storage. *J. Energy Storage* **2022**, *51*, 104568. [[CrossRef](#)]
14. Pirasaci, T. Investigation of phase state and heat storage form of the phase change material (PCM) layer integrated into the exterior walls of the residential-apartment during heating season. *Energy* **2020**, *207*, 118176. [[CrossRef](#)]
15. Royo, P.; Acevedo, L.; Ferreira, V.J.; García-armingol, T.; Ana, M.L. High-temperature PCM-based thermal energy storage for industrial furnaces installed in energy-intensive industries. *Energy* **2019**, *173*, 1030–1040. [[CrossRef](#)]
16. Prieto, C.; Cabeza, L.F. Thermal energy storage (TES) with phase change materials (PCM) in solar power plants (CSP). Concept and plant performance. *Appl. Energy* **2019**, *254*, 113646. [[CrossRef](#)]
17. Xu, B.; Li, P.; Chan, C. Application of phase change materials for thermal energy storage in concentrated solar thermal power plants: A review to recent developments. *Appl. Energy* **2015**, *160*, 286–307. [[CrossRef](#)]
18. Prieto, C.; Cabeza, L.F. Thermal energy storage with phase change materials in solar power plants. Economic analysis. *J. Energy Storage* **2021**, *43*, 103184. [[CrossRef](#)]
19. Gil, A.; Oro, E.; Miró, L.; Peiro, G.; Ruiz, Á.; Salmeron, J.M.; Cabeza, L.F. Experimental analysis of hydroquinone used as phase change material (PCM) to be applied in solar cooling refrigeration. *Int. J. Refrig.* **2014**, *39*, 95–103. [[CrossRef](#)]
20. Sellami, A.; Elotmani, R.; Kandoussi, K.; Eljoud, M.; Hajjaji, A.; Boutaous, M.H. Temperature regulation of PV solar cell under PCM cooling system. In Proceedings of the 2016 International Renewable and Sustainable Energy Conference (IRSEC), Marrakesh, Morocco, 14–17 November 2016; IEEE: Piscataway, NJ, USA, 2017.
21. Noro, M.; Lazzarin, R.M.; Busato, F. Solar cooling and heating plants: An energy and economic analysis of liquid sensible vs phase change material (PCM) heat storage. *Int. J. Refrig.* **2014**, *39*, 104–116. [[CrossRef](#)]
22. Zhang, D.; Li, C.; Lin, N.; Xie, B.; Chen, J. Mica-stabilized polyethylene glycol composite phase change materials for thermal energy storage. *Int. J. Miner. Metall. Mater.* **2022**, *29*, 168–176. [[CrossRef](#)]
23. Warner, J.; Liu, X.; Shi, L.; Qu, M.; Zhang, M. A Novel Shallow Bore Ground Heat Exchanger for Ground Source Heat Pump Applications—Model Development and Validation. *Appl. Therm. Eng.* **2019**, *164*, 114460. [[CrossRef](#)]
24. Zhang, M.; Liu, X.; Biswas, K.; Warner, J. A Three-Dimensional Numerical Investigation of a Novel Shallow Bore Ground Heat Exchanger Integrated with Phase Change Material. *Appl. Therm. Eng.* **2019**, *162*, 114297. [[CrossRef](#)]
25. Zhang, Y.; Liu, S.; Yang, L.; Yang, X.; Shen, Y.; Han, X. Experimental Study on the Strengthen Heat Transfer Performance of PCM by Active Stirring. *Energies* **2020**, *13*, 2238. [[CrossRef](#)]
26. Scharinger-Urschitz, G.; Walter, H.; Haider, M. Heat Transfer in Latent High-Temperature Thermal Energy Storage Systems—Experimental Investigation. *Energies* **2019**, *12*, 1264. [[CrossRef](#)]
27. Li, H.; Fan, L.; Geng, S.; Zhuang, K. The research on phase change heat storage air-conditioning reservoir for protective engineering. *Prot. Eng.* **2009**, *5*, 57–60.
28. Hou, P.; Mao, J.; Chen, F. Research on Application Schemes and Thermal Storage Characteristics of Phase Change Reservoir of Protective Engineering. *J. Refrig.* **2016**, *37*, 95–100.
29. Hou, P.M.; Mao, J.F.; Liu, R.R.; Chen, F. Design and Operating Characteristics of Heat Storage Device for Annular Unit. *J. Refrig.* **2018**, *39*, 98–107.
30. Crespo, A.; Zsembinszki, G.; Vérez, D.; Borri, E.; Fernández, C.; Cabeza, L.F.; de Gracia, A. Optimization of Design Variables of a Phase Change Material Storage Tank and Comparison of a 2D Implicit vs. 2D Explicit Model. *Energies* **2021**, *14*, 2605. [[CrossRef](#)]
31. Zhang, H.; Lu, J.; Zhuang, C.; Huang, G.; Yu, J.; Liu, Y. Performance of the Phase Change Heat Storage Air-Conditioning Reservoir for Underground Protective Engineering. *J. Tianjin Univ.* **2019**, *52*, 1187–1193.
32. Niyas, H.; Prasad, S.; Muthukumar, P. Performance investigation of a lab-scale latent heat storage prototype—Numerical results. *Energy Convers. Manag.* **2017**, *135*, 188–199. [[CrossRef](#)]
33. Tao, W. *Numerical Heat Transfer*, 2nd ed.; Xi'an Jiaotong University Press: Xi'an, China, 2001.
34. Li, Z.; Zhang, S. Research Progress and Application of Phase Change Materials. *Build. Energy Effic.* **2016**, *44*, 57–60.
35. Wang, S.; Ling, F.; Sun, J.; Yan, Y.; Li, L. Research Progress and Thermal Properties of Wax Composite Phase Change Materials. *Contemp. Chem. Ind.* **2015**, *44*, 1598–1601.